Renewable and Sustainable Energy Reviews 60 (2016) 1615–1633

Contents lists available at ScienceDirect

Renewable and Sustainable Energy Reviews

journal homepage: www.elsevier.com/locate/rser

A review on the heat and mass transfer phenomena in nanofluid coolants with special focus on automotive applications

Masoud Bozorg Bigdeli [a,b], Matteo Fasano [a], Annalisa Cardellini [a], Eliodoro Chiavazzo [a,*], Pietro Asinari [a]

[a] Dipartimento di Energia, Politecnico di Torino, Corso Duca degli Abruzzi 24, 10129 Torino, Italy
[b] Department of Mechanical Engineering, University of Alberta, Edmonton, AB, T6G 2G8, Canada

ARTICLE INFO

Article history:
Received 19 March 2015
Received in revised form
25 January 2016
Accepted 4 March 2016
Available online 25 March 2016

Keywords:
Nanofluid coolants
Nanocolloids for thermal engineering
Sustainable energy devices
Automotive coolants
Enhanced heat transfer

ABSTRACT

Engineered suspensions of nanosized particles (nanofluids) may be characterized by enhanced thermal properties. Due to the increasing need for ultrahigh performance cooling systems, nanofluids have been recently investigated as next-generation coolants for car radiators. However, the multiscale nature of nanofluids implies nontrivial relations between their design characteristics and the resulting thermo-physical properties, which are far from being fully understood. In this work, the role of fundamental heat and mass transfer mechanisms governing thermo-physical properties of nanofluids is reviewed, both from experimental and theoretical point of view. Particular focus is devoted to highlight the advantages of using nanofluids as coolants for automotive heat exchangers, and a number of design guidelines are reported for balancing thermal conductivity and viscosity enhancement in nanofluids. We hope that this review may help further the translation of nanofluid technology from small-scale research laboratories to industrial application in the automotive sector.

Contents

Abbreviation: BG, Bruggeman; CMC, critical micelle concentration; CNT, carbon nanotube; DLVO, Derjaguin, Landau, Verwey, and Overbeek; DSC, differential scanning calorimetry; EDL, electric double layer; EG, ethylene glycol; EO, engine oil; HC, Hamilton-Crosser; IEP, isoelectric point; MG, Maxwell–Garnett; MWCNT, multi-walled carbon nanotube; NTU, number of heat transfer units; OA, oleic acid; SSA, specific surface area

* Corresponding author.
E-mail address: eliodoro.chiavazzo@polito.it (E. Chiavazzo).

http://dx.doi.org/10.1016/j.rser.2016.03.027
1364-0321/

1. Introduction

In automotive liquid-cooled engines, radiator is a compact heat exchanger coupled to channels distributed throughout the cylinder heads and engine, through which the coolant is pumped. Different methods have been proposed to enhance the heat transfer performance of car radiators, and they can be classified into active and passive techniques [1,2]. While active methods require power supply (e.g. mechanical mixing), passive enhancement techniques are not dependent on external sources and thus are characterized by lower operating costs and higher reliability, especially with compact energy devices [3,4,259].

Among other passive methods such as fins, engineered surface texturing and microchannels [5–9], the adoption of novel coolants with enhanced thermo-physical properties as compared to conventional ones (e.g. water, oil, ethylene glycol) has attracted interest in the automotive field for a long time [10–16]. As a matter of fact, early scientists tried to suspend millimeter- and micrometer-sized particles with high thermal conductivity in traditional coolants to improve their thermal properties. However, due to the associated high pressure drop, clogging of flow channels and corrosion of the components (heat exchangers, pipelines, pumps), the approach was initially considered inappropriate. Later on, advancements in colloid and interface science along with improvements in powder manufacturing techniques resulted in the synthesis of colloidal suspensions of nanosized particles with enhanced transport properties, called nanofluids [17,18].

In the past decades, nanofluids have been proposed for a wide variety of applications. In the engineering field, nanofluids have been mainly indicated as novel coolants for both electronic [19,20] and automotive components [21–27], with the potential to reduce the dimensions of traditional heat exchangers. Nanofluids have also mechanical applications as magnetic sealants [28] or lubricants [29,30], and energy applications in solar water heaters [21,31]. More generally, nanofluids also show great potential in the biomedical sector, especially in antibacterial [32], nanocryosurgery [33] or theranostic [34,35] applications.

The growing interest of automotive industry on nanofluid coolants is witnessed by the exponential increase of published patents and by market reports, which are indicating nanofluids as one of the key trends and drivers in the car radiator industry in the period 2014–2020 [36]. The main advantage of nanofluids for automotive cooling systems is the high thermal conductivity of solid nanoparticles, which can be hundreds or thousands times greater than the one of conventional heat transfer fluids [37,38]. Therefore, nanofluids containing a small amount of uniformly and stably dispersed nanoparticles can provide a considerable enhancement in thermal conductivity (e.g. up to 30% increase with TiO_2–water suspensions [39,40]) when compared to base fluids, such as water, ethylene glycol, engine oil or ethanol [41,42]. However, the increased thermal conductance of nanofluids is often accompanied by increased viscosity and corrosion of mechanical components, therefore limiting a wider commercial exploitation of nanofluids in automotive applications [1].

If nanofluids are used as coolants in car radiators, a number of thermo-physical properties have to be taken into account for evaluating their overall cooling efficiency, namely thermal conductivity, specific heat capacity, density and viscosity [43]. This is because they strongly influence the characteristic thermal transmittance and inertia of the nanofluid as well as the required pumping power, respectively. However, an overall guideline for automotive engineers to provide them with the necessary tools to systematically analyze the influence of nanoparticles and base fluid parameters on the effective thermo-physical properties of nanofluid coolants, and subsequently on the engine performance, is still missing.

Thus, the approach towards the production of highly efficient engines necessitates the introduction of innovative cooling technologies, such as nanofluid coolants. However, it is essential to consider the effect of both increased thermal conductivity and viscosity to evaluate the global energy performance of nanofluid coolants. To this purpose, this review aims at rationalizing the experimental, computational and physical evidences on the heat and mass transfer phenomena observed in nanofluids. Furthermore, the potential heat transfer enhancement offered by nanofluids as novel coolants for automotive applications is critically reviewed. Finally, the challenges to harnessing the benefits of this technology are discussed and perspectives for further development of nanofluid technology are suggested.

2. Nanofluid synthesis

Nanofluids are suspensions of nanoparticles (diameter $d_p \leq 100$ nm) immersed in a host fluid, which is also referred to as base fluid. Thermo-physical properties of nanofluids depend on the characteristics of base fluid and nanoparticles, which are both influenced by fabrication techniques. Nanoparticles are typically made out of a solid core and a shell or coating, which is chemically bonded or adsorbed on its surface. Generally, the nanoparticle core defines the main characteristics of the particle, such as thermal, electric, magnetic and optical properties, whereas the nanoparticle coating defines the stability of the particle suspension as well as the hydrophilic or hydrophobic behavior and the interfacial Kapitza thermal resistance [44].

Thermo-physical properties of nanofluids have a strong dependence on the characteristics of host fluid [45]. Fluids like water, ethylene glycol, engine oil or a mixture of them are typically used for experiments on vehicle cooling systems [23,26]. According to the hydrophilic or hydrophobic properties of both nanoparticle and host fluid, proper coatings and stabilizers should be employed to obtain stable suspensions [46].

Typical materials of nanoparticle core are ceramic (CuO, Al_2O_3, TiO_2, SiC, SiO_2, Fe_3O_4, ZnO), metallic (Cu, Al, Ag, Au, Fe) or carbon-based (carbon nanotube, graphene), whereas coatings may have molecular or polymeric composition [47–50]. Particle coatings may be in turn composed of an active head and a tail group, as schematically reported in Fig. 1. Generally, the active head group binds to the nanoparticle surface by creating chemical bonds: the

Nomenclature

Roman symbols

ΔP	pressure drop (Pa)
$\dot{Q}$	heat transfer rate (W)
$\dot{V}$	volumetric flow rate (m^3/s)
$\dot{m}$	mass flow rate (kg/s)
AR	aspect ratio (–)
D_h	hydraulic diameter (m)
L_r	radiator length (m)
Nu	Nusselt number (–)
Pr	Prandtl number (–)
R_k	Kapitza resistance (m^2 K/W)
Re	Reynolds number (–)
T	temperature (°C)
U_r	overall heat transfer coefficient of the radiator (W/m^2 K)
V_r	total radiator volume (m^3)
V	volume (m^3)
W	pumping power (W)
c_p	specific heat capacity (J/kg K)
d_{bf}	base fluid molecule diameter (m)
d_p	particle diameter (m)
f	friction factor (–)
h	heat transfer coefficient (W/m^2 K)
k_B	Boltzmann constant (J/K)
k	thermal conductivity (W/m K)
l_k	Kapitza length (m)
n	shape factor (–)
r_p	particle radius (m)
u	velocity (m/s)

Greek symbols

β	thermal expansion coefficient (K^{-1})
δ	nanolayer thickness (m)
ϵ	heat exchanger effectiveness (–)
η	efficiency (–)
η_0	total surface effectiveness (–)
μ	viscosity (Pa s)
ϕ	volume fraction (–)
ϕ_{int}	volume fraction of particles in the aggregates (–)
ψ	sphericity (–)
ρ	density (kg/m^3)

Subscripts

bf	base fluid
fr	freezing point
FT	flat tube
in	tube inlet
nf	nanofluid
pe	equivalent particle
p	particle
RT	round tube
r	ratio

Chemical formulas

SDBS	sodium dodecyl benzene sulfonate
SDS	sodium dodecyl sulfate

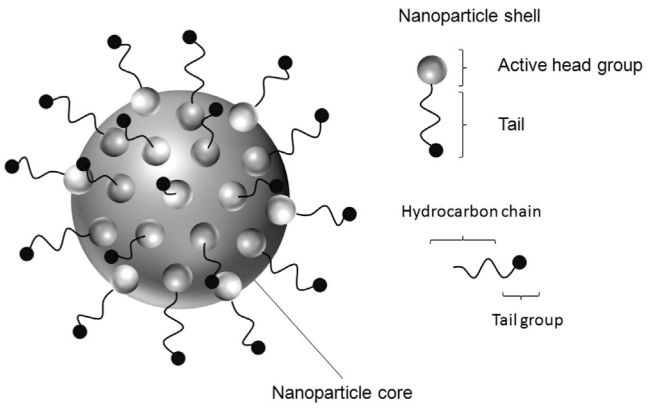

Fig. 1. Schematic of a typical nanoparticle structure. Figure reproduced based on reference [47].

stronger the chemical bonds are, the harder they tend to dissociate from the surface. This induces more stable nanofluid properties. The tail group, instead, is usually composed of two parts: a hydrocarbon chain and an ending tail. The tail group interacts with the dispersion medium, thus promoting a good dispersion of nanoparticles.

For instance, carbon nanotubes (CNTs) possess hydrophobic surface properties and, therefore, are prone to aggregation and sedimentation in aqueous media. For better stability in water, surface properties of CNTs are usually modified by introducing proper stabilizers, such as Sodium Dodecyl Sulfate (SDS) [51,52]. On the other hand, metallic and ceramic nanoparticles are generally characterized by hydrophilic surface properties, and therefore they should be functionalized for synthesizing stable oil-based nanofluids. Choi et al. [53] treated the Al_2O_3 nanoparticle surface by Oleic Acid (OA) through a hydrophobic modification process to prepare an oil-based nanofluid. As another example, Shima and Philip [54] modified Fe_3O_4 and Ag nanoparticles surfaces by Oleic Acid and Oleylamine, respectively, in order to prepare hexadecane-based nanofluids.

Two main methods are currently adopted for synthesizing nanofluids: single-step and two-step processes. In general, single-step synthesis is more reliable for producing metallic nanofluids, since it prevents particle oxidation. On the contrary, the two-step technique is preferable for the synthesis of ceramic-based (e.g. oxides, carbides) nanofluids [46,55].

Single-step synthesis can be performed by either physical [56] or chemical methods [57]. Introduced by Akoh et al. [56], the single-step physical synthesis involves the direct condensation of metallic vapor into nanoparticles by contact with a low vapor pressure fluid flow [58]. Generally, single-step processes directly synthesize nanoparticles in the base fluid, thus avoiding the processes of drying storage, transportation and re-dispersion of the metallic nanoparticles [57,59]. Normally, physical vapor deposition [56,58], solution chemical method [57] or microwave-assisted route [60,61] are adopted for single-step synthesis of nanofluids. These methods usually minimize agglomeration of particles in the nanofluid and thus enhance its stability. However, single-step methods introduce a limit to the nanofluid production quantities, because only low vapor pressure liquids are currently compatible with these processes [62,63].

Two-step methods are also widely used for the synthesis of nanofluids. In these processes, the dry nanopowders available from different physical and chemical methods (e.g. inert gas condensation [64], chemical vapor deposition [65,66], physical vapor deposition [67] or mechanical alloying [68]) are dispersed into a base fluid [69–72]. Currently, the two-step approach is the cheaper method for large scale production of nanofluids, since nanopowder synthesis techniques have already been scaled up to industrial production levels. Moreover, two-step processes are widely adopted also because of the possibility to precisely and easily control the concentration and size distribution of the solvated nanoparticles [73,74]. The main drawback of two-step techniques is the higher possibility of particle agglomeration due to attractive van der Waals interactions [55,75].

Ultrasonic agitation as well as pH adjustment or introduction of surfactants may be required to obtain stable suspensions [69,72,76,77]. In detail, surface active agents (i.e. surfactants) are molecular structures with amphiphilic nature (i.e. coexistence of hydrophobic and hydrophilic molecular portions [78]), which makes them ideal stabilizers for nanofluids with aqueous or oleic phases. Surfactants can be introduced either during the fabrication process (two-step processes, Fig. 2) or directly into the synthesized nanofluid (single-step processes).

3. Dominating heat and mass transfer mechanisms

The multiscale nature of nanofluids leads to nontrivial relations between their geometrical, physical and chemical characteristics and the resulting thermo-physical properties. This pronounced sensitivity is the main reason for some contradictory results among both experimental evidence and theoretical considerations presented in the literature.

In particular, classic effective medium theory has been modified to take into account the structured solid-like layer of water molecules at the nanoparticle–fluid interface (i.e. nanolayer) [79–88,260,261]. Moreover, Brownian motion [89–94], interfacial thermal resistance (i.e. Kapitza Resistance) [95] and the formation of thermal percolation paths due to particle aggregation [96] were also proposed for understanding the anomalous thermal properties of nanofluids [38,97–99]. After several experiments and some controversies, it is now well recognized that the two main features characterizing the effective thermal conductivity of nanofluids are the Kapitza resistance at the nanoparticle–fluid interface [100] as well as the role of aggregation and aggregate morphologies [101]. In particular, it is nowadays accepted that chain-forming morphologies of nanoparticles allow effective medium theories to predict thermal conductivity enhancements [102]. As a counter example, a large round-robin test on nanofluids proved that ideal dispersion cancels out any meaningful enhancement [103].

Experimental data corresponding to thermal conductivity of nanofluids largely fall within the lower and upper Maxwell bounds derived by Hashin and Shtrikman [104]. Most enhancements beyond predictions of effective medium theories come from thermal percolating effects due to aggregation of nanoparticles (see Fig. 3, where k_{nf} and k_{bf} are thermal conductivities of nanofluid and base fluid, respectively) [99]. The only way to benefit from the aggregation of nanoparticles while avoiding its negative effects is to have control over the entire process and keep aggregation at controlled levels. This is of prominent importance in automotive cooling circuits, as uncontrolled aggregation may lead to clogging of tubes. Understanding the nature of interaction forces between nanoparticles may pave the way to achieve control over this process.

Hence, the study of aggregate morphologies and dynamics is currently a central topic in colloidal science. The key tool for the molecular investigation of particle aggregation mechanisms is the effective interaction potential between nanoparticles, which can be qualitatively described by the well-known DLVO theory (due to Derjaguin, Landau, Verwey and Overbeek) [107–109]. However, it is nowadays recognized that additional forces (so-called non-DLVO forces) play a major role in determining the colloidal stability [110]. Solvation forces, for example, can arise when liquid molecules are induced to order in the nanoscale gaps between approaching nanoparticles; however, fundamental theories are still missing for a more quantitative prediction of non-DLVO forces and thus aggregation phenomena [110].

4. Thermal properties of nanofluids

Thermal conductivity (k_{nf}), specific heat capacity ($c_{p,nf}$) and thermal expansion (β_{nf}) can be considered as the main quantities for evaluating the overall thermal performance of nanofluids. Typically, thermal conductivity of nanofluids is larger than that of the base fluid, whereas specific heat capacity is smaller. In this section, thermal properties of nanofluids are reviewed from experimental, modeling and theoretical point of view.

4.1. Thermal conductivity

4.1.1. Experimental evidences

Several techniques have been proposed for measuring thermal conductivity of nanofluids, namely transient methods, steady-state methods and the thermal comparator technique [111]. Transient approaches include transient hot-wire technique [39,112–116], thermal constants analyzer [117,118], temperature oscillation [119,120] and the 3ω method [121]. Steady-state parallel-plate [122] and cylindrical cell [123] can be instead classified as steady-state techniques. Among these methods, transient hot-wire

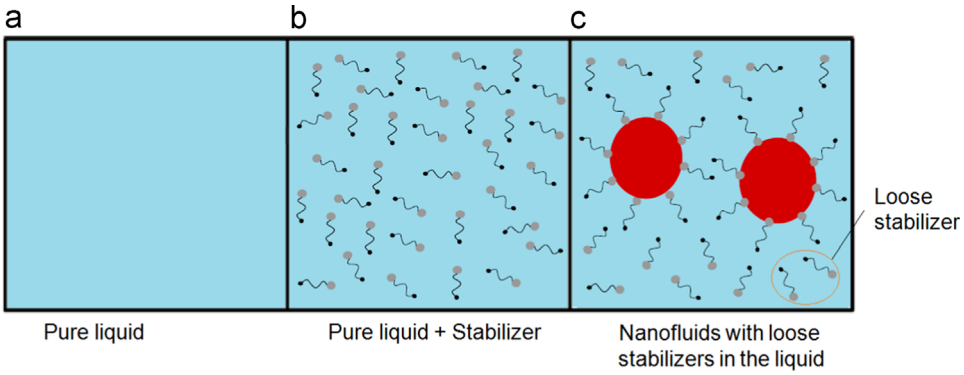

Fig. 2. Two-step fabrication of nanofluids using stabilizers. Figure reproduced based on reference [1].

technique is the most adopted solution. Noteworthy, Li et al. [124] compared results from transient and steady-state thermal conductivity measurements in a Al_2O_3–water nanofluid. Results revealed that both methods led to similar thermal conductivity values at room temperature; whereas, by increasing temperatures, a significant discrepancy between the methods was evident. This was due to the onset of natural convection in the hot-wire setup [125].

Experimental analyses on thermal conductivity of nanofluids have shown several non-trivial characteristics. First, opposite trends are noticeable regarding the relation between thermal conductivity and decreasing particle size: (1) a decrease of thermal conductivity because of the increase in the overall solid–liquid interface effects [45,126–131] (Fig. 4); (2) an increase of thermal conductivity because of the nanolayer effect and the increase of random motion of nanoparticles, which promotes the creation of percolation paths [89,98,132–134].

Second, the pH of nanoparticle suspensions strongly affects the nanofluid stability and its thermo-physical properties. For heat transfer purposes, it is generally recommended to synthesize suspensions with pH values far from isoelectric point (IEP), in order to avoid severe aggregation of nanoparticles [135]. Some studies underline an enhancement in thermal conductivity around the IEP [136–138], which could be due to the partial aggregation of particles and subsequent formation of thermal percolation pathways [98,132,133]. Therefore, a partial and controlled aggregation of nanoparticles, which can be adjusted by either pH tuning or surfactant addition, may enhance the thermal properties of nanofluids [77,139–141].

Third, several experimental works report $k_r = k_{nf}/k_{bf}$ as a function of surfactant concentration. Based on these studies, there exists an optimum value at which k_r is maximum, as depicted in Fig. 5 [77,118]. On one hand, this enhancement is due to a better dispersion of nanoparticles within the base fluid; on the other hand, it could be also attributed to nanolayer formation [117,118].

Finally, thermal conductivity may show nonlinear behavior with particle concentration [142,143], temperature dependence [119,144–149] and the possibility to be tuned by external fields [150,151].

Thermal conductivity values for a selection of nanoparticles, base fluids and nanofluids of interest for automotive applications are reported in Tables 1, 2, and 3, respectively.

4.1.2. Semi-empirical models

Starting from experimental evidences, scientists have tried to semi-empirically model the relation between nanofluid characteristics and resulting thermal conductivity. For instance, the experimental model developed by Patel et al. [153] for spherical metallic and oxide nanoparticle suspensions is:

$$k_r = \left(1 + 0.135 \times \frac{k_p}{k_{bf}}^{0.273} \times \phi^{0.467} \times \frac{T}{20}^{0.547} \times \frac{100}{d_p}^{0.234}\right), \quad (1)$$

where T is the nanofluid temperature.

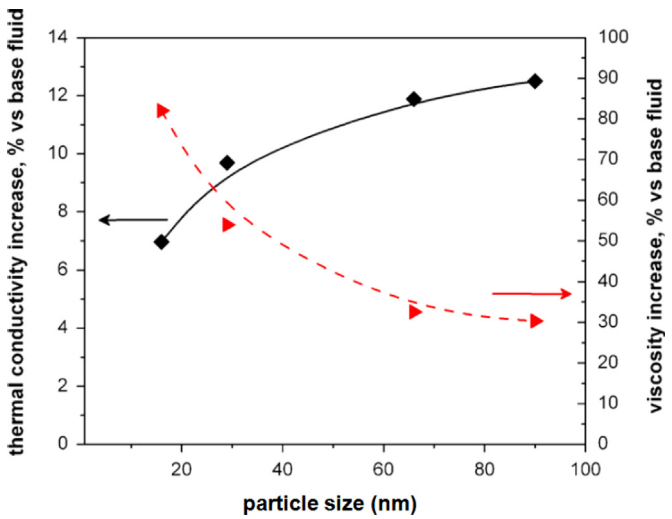

Fig. 4. Dependence of thermal conductivity and viscosity of α-SiC-water nanofluids on the particle size (T=22.5 °C, ϕ = 0.041, pH=9.4). The black line and diamonds represent the dependence of k_r on d_p, whereas the red dashed line and triangles represent the dependence of μ_r on d_p. Figure adopted from reference [130].

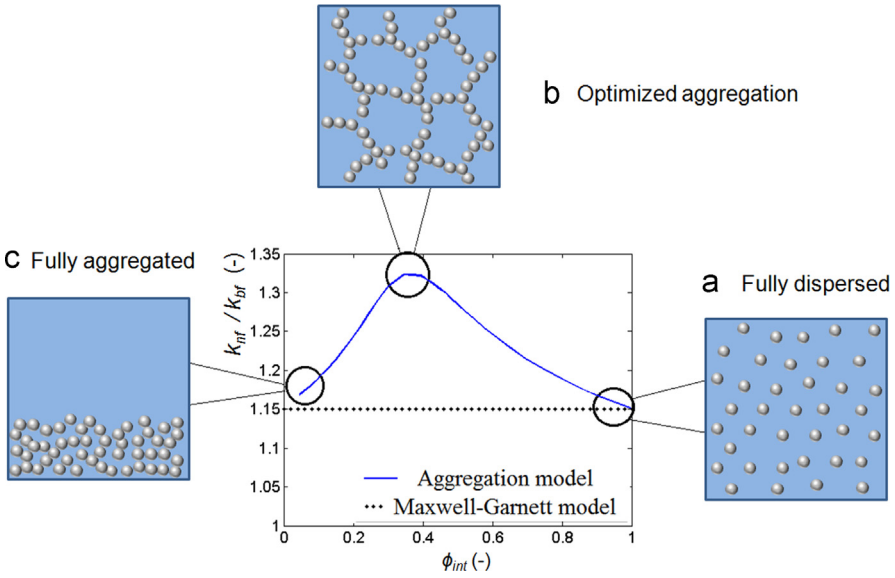

Fig. 3. Aggregation dependence of thermal conductivity enhancement in nanofluids. (a) For a well-dispersed system, there is only one particle in each aggregate ($\phi_{int} = 1$) and the thermal conductivity is in accordance with effective medium theory (Maxwell-Garnett model [105]). (b) As particles tend to aggregate, the thermal conductivity of the suspension increases (diverges from Maxwell-Garnett model) and experiences a maximum value at optimized aggregation state. (c) Further aggregation increase leads to lower thermal conductivity values, until the system is fully-aggregated. Figure reproduced based on references [1,98,106].

In another work, Corcione [161] proposed an empirical model based on data extracted from experimental studies:

$$k_r = 1 + 4.4 Re^{0.4} Pr^{0.66} \left(\frac{T}{T_{fr}}\right)^{10} \left(\frac{k_p}{k_{bf}}\right) \phi^{0.66}, \quad (2)$$

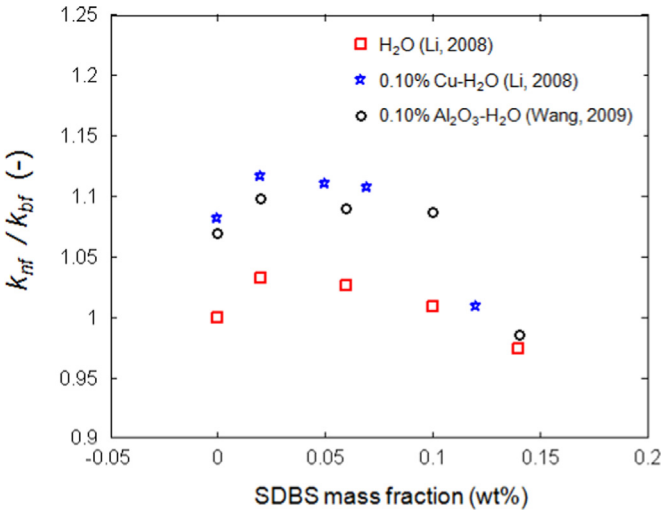

Fig. 5. Effect of SDBS concentration on thermal conductivity of Cu- and Al_2O_3-water based nanosuspensions. Blue stars, black circles and red squares represent Al_2O_3-water suspensions, Cu-water suspensions and pure water, respectively. Figure is reproduced based on reference [118].

Table 1
Thermal conductivity (W/mK) of particle materials at 300 K.

Material	Thermal conductivity (W/mK)	References
MWCNT	3000	[48,152]
Ag	429	[37,152]
Cu	383–401	[153,37]
Al	204–237	[153,152]
Si	148	[37,152]
SiC	120–490	[152,154,140]
CuO	18–76.5	[153,155,156]
Al_2O_3	40	[48]
SiO_2	1.38	[156]

Table 2
Thermal conductivity (W/mK) of heat transfer fluids at 27 °C (unless otherwise noted). Water–EG is a 50:50 wt% mixture of water and ethylene glycol.

Fluid	Thermal conductivity (W/mK)	References
Water	0.613	[37,152]
EG	0.253	[152]
EO	0.145	[37,152]
Water–EG	0.403	[76,157]
Water–EG at 90 °C	0.422	[76]

where Re is the Reynolds number for the Brownian motion of nanoparticles, Pr is the Prandtl number of the base fluid and T_{fr} is the freezing point of the base fluid. This model is valid for water and ethylene glycol based nanofluids containing alumina, copper oxide, titania or copper nanoparticles. Re can be evaluated as:

$$Re = \frac{\rho_{bf} u_B d_p}{\mu_{bf}}, \quad (3)$$

where u_B and μ_{bf} are the mean Brownian velocity of the nanoparticle and the viscosity of the base fluid, respectively; whereas Pr is defined as:

$$\mathrm{Pr} = \frac{c_{p,\mathrm{bf}} \mu_{\mathrm{bf}}}{k_{\mathrm{bf}}}, \quad (4)$$

where $c_{p,bf}$ is the specific heat capacity of the base fluid.

Chon et al. [162], instead, proposed an experimental correlation for the thermal conductivity of Al_2O_3 nanofluids based on Buckingham–Pi theorem:

$$k_r = 1 + 64.7 \phi^{0.7460} \left(\frac{d_{bf}}{d_p}\right)^{0.3690} \times \left(\frac{k_p}{k_{bf}}\right)^{0.7476} \times Pr^{0.9955} Re^{1.2321}, \quad (5)$$

where d_{bf} is the base fluid molecule diameter.

Timofeeva et al. [163] experimentally proved that Kapitza resistance increases with decreasing particle sphericity, because of enhanced interfacial effects. Thus, they modeled the thermal conductivity of nanofluids by considering the effects of shape and thermal boundary resistance, namely:

$$k_r = 1 + (C_K^{shape} + C_K^{surface})\phi, \quad (6)$$

where C_K^{shape} is the contribution due to particle shape and $C_K^{surface}$ the contribution due to the Kapitza resistance (Fig. 6). Based on this study, it is possible to define an upper limit for the shape factor of nanoparticles above which the limiting effect due to Kapitza resistance increases faster than the positive contribution by particle shape, namely $n < 5$.

4.1.3. Theoretical models

To provide a mechanistic explanation of the thermal conductivity enhancement in nanofluids, various theoretical models based on classic effective medium theory (EMT) have been introduced, and some of them are discussed here.

The Maxwell–Garnett (MG) model [105] predicts the thermal conductivity enhancement (k_r) for a homogeneous suspension as:

$$k_r = \frac{k_{nf}}{k_{bf}} = \frac{k_p + 2k_{bf} + 2(k_p - k_{bf})\phi}{k_p + 2k_{bf} - (k_p - k_{bf})\phi}, \quad (7)$$

where k_p is the particle thermal conductivity, whereas ϕ is the particle volume fraction. Note that, the maximum heat conduction enhancement ($k_{r_{max}}$) is obtained for $k_p \gg k_{bf}$. This condition represents the upper limit for thermal conduction enhancement within the macroscopic theory [116], namely:

$$k_{r_{max}} = \frac{1 + 2\phi}{1 - \phi} \approx 1 + 3\phi. \quad (8)$$

Table 3
Thermal conductivity experimentally measured in nanofluids.

Nanofluid	Particle diameter (nm)	Particle length (nm)	ϕ (%)	Temperature (°C)	k_{nf} (W/mK)	References
Al_2O_3–water	40	–	10	23	0.734	[158]
Al_2O_3–EG	40	–	10	23	0.312	[158]
Al_2O_3–water/EG	10	–	2.9	23	0.468	[76]
CuO–water	29	–	12	21–23	0.70	[147]
DWCNT–water	3.5	$(1-10) \times 10^3$	0.14	–	0.8778	[159]
SWCNT–water	1	100–600	0.2	60	0.756	[160]
SWCNT–EG	1	100–600	0.2	55	0.358	[160]

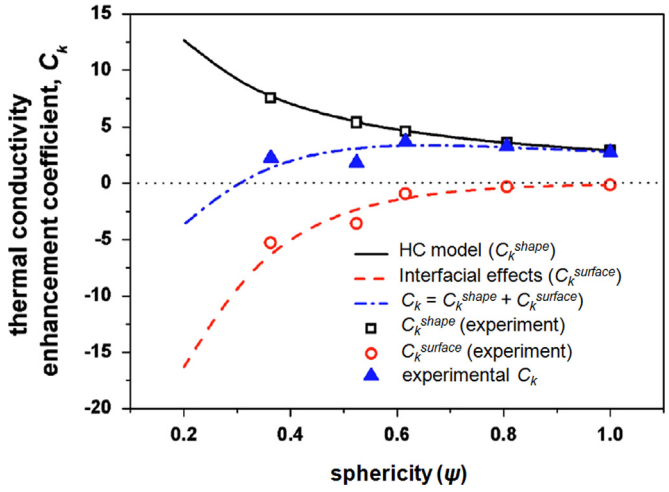

Fig. 6. Contribution of particle shape and interfacial thermal resistance to the thermal conductivity of nanofluids at various particle sphericity (ψ). Black solid, red dashed and blue dash-dotted lines represent the Hamilton and Crosser - HC model, the trend of interfacial effects and the overall influence of shape and interface properties, respectively. Black squares, red circles and blue triangles represent the experimental evaluation of particle shape effect (C_k^{shape}), particle surface effect ($C_k^{surface}$) and their overall influence on thermal conductivity enhancement (C_k), respectively. Figure adopted from reference [163].

The MG model holds for low concentrations of not interacting spherical particles; therefore, it does not interpret experimental results at high volume concentrations. On the contrary, the Bruggeman model (BG) has no limitation on the spherical particles concentration, and it accounts for interactions among particles. This model can be expressed as:

$$\phi\left(\frac{k_p - k_{nf}}{k_p + 2k_{nf}}\right) + (1-\phi)\left(\frac{k_{bf} - k_{nf}}{k_{bf} + 2k_{nf}}\right) = 0. \tag{9}$$

Note that, for low volume fractions, MG and BG models lead to approximately equal results [164,165].

The Maxwell–Garnett model only considers volume concentration and thermal conductivity of particles and base fluid. Starting from MG relation, Hamilton and Crosser (HC) [166] developed a model also taking into account the particle shape:

$$k_r = \frac{k_p + (n-1)k_{bf} - (n-1)(k_{bf} - k_p)\phi}{k_p + (n-1)k_{bf} + (k_{bf} - k_p)\phi}, \tag{10}$$

where $n = 3/\psi$ is the shape factor and ψ the particle sphericity. The latter is defined as the ratio between the equivalent sphere surface and the actual particle surface, at fixed volume [163].

The MG and HC models are accurate to order ϕ^1. Jeffrey [167] extended the accuracy of these models to ϕ^2 for spherical nanoparticles, namely:

$$k_r = 1 + 3\beta\phi + \phi^2\left(3\beta^2 + \frac{3\beta^2}{4} + \frac{9\beta^3}{16}\frac{\alpha+2}{2\alpha+3} + \frac{3\beta^4}{2^6} + \ldots\right), \tag{11}$$

where $\alpha = k_p/k_{bf}$ and $\beta = (\alpha-1)/(\alpha+2)$.

Further theoretical models were developed to explain the heat conduction behavior of nanofluids, thus giving rise to controversies and mismatch between experimental evidences and modeling interpretations [119,144,146,149,153,158,168,169].

4.2. Other thermal properties

4.2.1. Specific heat capacity

Specific heat capacity, c_p, has received little attention if compared to the thermal conductivity and viscosity of nanofluids. However, this quantity has an important role to define the thermal performance of nanofluids in cooling applications (see Section 6), as it is incorporated into the energy equation [170,171].

Differential Scanning Calorimeter (DSC) is recognized as the standard technique for measuring the specific heat capacity of fluids and materials. DSC technique has been successfully implemented in a large number of nanofluid studies [172–178]. Alternatively, some researchers suggested their own experimental setups for measuring c_p of nanofluids [8,179,180].

In experiments, the specific heat capacity of nanofluids ($c_{p,nf}$) is found to be influenced by several parameters, including particle volume or weight fraction [69,173,174,176,177,179,181–183], temperature [176,177,181,182,184], particle size and shape [185], particle material [186], and base fluid type [186].

For instance, in the case of alumina nanoparticles in water, the increase in particle volume fraction induces a $c_{p,nf}$ decrease, because the specific heat capacity of alumina particles is lower than c_p of water [179,187]. However, in case of carbon nanotubes (CNTs) in ethylene glycol (EG) the opposite behavior is observed, due to the higher specific heat capacity of CNT particles compared to that of EG [187,188]. With respect to the particle size effect, Wang et al. [185] showed that $c_{p,p}$ (specific heat capacity of nanoparticles) depends on the size and shape of nanoparticles. Hence, it is also possible to tune $c_{p,nf}$ by adjusting nanoparticles' geometry.

Starting from the experimental data of Al_2O_3, SiO_2, and ZnO nanofluids, Vajjha and Das [179] developed a general correlation for $c_{p,nf}$:

$$c_{p,r} = \frac{c_{p,nf}}{c_{p,bf}} = \frac{(AT) + B\left(\frac{c_{p,p}}{c_{p,bf}}\right)}{C + \phi}, \tag{12}$$

where $c_{p,r}$ is the specific heat capacity ratio and A, B, C are fitting coefficients (see reference [179]). The latter correlation predicts the specific heat capacity of nanofluids for concentrations up to either 10% (Al_2O_3 and SiO_2 nanoparticles) or 7% (ZnO nanoparticles), within the temperature range of 315–363 K [179].

Two theoretical models based on mixing rules are generally adopted to predict the effective heat capacity of nanofluids ($c_{p,nf}$). Pak and Cho [69] introduced the first model, namely:

$$c_{p,nf} = (1-\phi)c_{p,bf} + \phi c_{p,p}. \tag{13}$$

Therefore, in the case of aqueous nanofluids, $c_{p,nf}$ is reduced by increasing the nanoparticle volume concentration.

Assuming that nanoparticles and base fluid are in thermal equilibrium, Xuan and Roetzel [189] suggested a second model [189]:

$$c_{p,nf} = \frac{(1-\phi)(\rho c_p)_{bf} + \phi(\rho c_p)_p}{\rho_{nf}}, \tag{14}$$

where $(\rho c_p)_{bf}$ and $(\rho c_p)_p$ are the volumetric heat capacities of base fluid and nanoparticles, respectively, and ρ_{nf} is the nanofluid density. The latter model accurately predicts most experimental results and, hence, it is usually employed in nanofluid studies [180,190,191].

For extended reviews regarding the typical nanofluids specific heat capacity, the reader is delegated to references [175,179,190,192].

4.2.2. Thermal expansion

The characteristic thermal expansion of a fluid also affects its heat transfer performances. Two theoretical models are widely used for predicting the effective thermal expansion coefficient of nanofluids (β_{nf}).

The first model is:

$$\beta_{nf} = (1-\phi)\beta_{bf} + \phi\beta_p, \tag{15}$$

where β_{bf} and β_p are the base fluid and nanoparticle thermal expansion coefficients, respectively [193]. In the second model, β_{nf} is approximated by a density-weighted average of particle and base fluid properties [194], namely:

$$\beta_{nf} = \frac{(1-\phi)(\rho\beta)_{bf} + \phi(\rho\beta)_p}{\rho_{nf}}, \tag{16}$$

where ρ_{bf} and ρ_p are base fluid and nanoparticle density, respectively. Note that Eqs. (15) and (16) are analogous to the models adopted for the specific heat capacity of nanofluids, namely Eqs. (13) and (14).

However, these models are sometimes insufficient to accurately interpret experiments. For instance, Ho et al. [195] experimentally measured β_{nf} of alumina–water nanofluids at different volume fractions, finding that neither Eq. (13) nor (14) could fit well the ϕ–β relation [165].

5. Fluid dynamic properties of nanofluids

Fluid dynamic properties of nanofluids are other important factors to be considered in heat transfer applications. In this section, the relation between nanofluid characteristics, viscosity and density is reviewed.

5.1. Viscosity

5.1.1. Experimental evidences

Viscosity is usually measured by rotational [196], capillary [197] or piston-type [198] viscometers.

Rotational viscometers evaluate the fluid viscosity by measuring the torque required to turn an object in that fluid. Using this viscometer, the viscosity of both Newtonian and non-Newtonian fluids can be measured. However, the time consuming procedure ($\approx$1 hour per sample) and the relatively large amount of sample consumptions ($\approx$1 mL per test) are the main drawbacks of employing rotational viscometers [199]. Moreover, classic models for the nanofluid viscosity [200,201] often underpredict measurements by rotational viscometers [202]. Some researchers argued that the difference between theoretical expectations and experimental results is associated with the low measurement accuracy of rotational viscometers, at least with nanofluid samples [202–204].

Therefore, capillary viscometers with different tube diameters are preferred in several experimental studies [202,203]. The main drawback of capillary viscometers is the possible dependence of viscosity on the particle-to-tube ratio [203]. Furthermore, the uncertainties in the measurement of tube diameter size, pressure drop and flow rate may affect the overall accuracy of capillary viscometers [202,204].

Experimental evidences on nanofluid viscosity (μ_{nf}) have shown a strong dependence on the physical and chemical properties of the suspensions, such as nanoparticle size and shape [63,130,163,205–207], solid phase volume concentration [163,208–210], pH of the solution [136,211], surfactant concentration [78,212–215] and temperature of the suspension [198,216].

In particular, controversial trends concerning the effect of particle size on the effective viscosity of nanofluids are reported in the literature. Some scientists notice the increase of viscosity by reducing the particle size (Fig. 4) [45,130,217–219], whereas other studies report an opposite trend [198,220]. The existence of these contradictory results could be due to several factors, such as different nanofluid preparation or measuring techniques, as well as presence of different surfactants, pH, temperature or agglomeration during the experiments [63,130].

Extended reviews regarding experimental viscosity of nanofluids can be found in references [63,210,216,221–225].

5.1.2. Semi-empirical models

Numerous empirical models have been formulated to interpret experimental results of nanofluids viscosity [165,198,218,226–228].

For example, Yang et al. [172] studied the temperature dependence of viscosity, experimentally proving that viscosity decreases with increasing temperatures. In addition, Namburu et al. [229] observed that, in the range −35 to 50 °C, the viscosity of a nanofluid made out of CuO nanoparticles suspended in a 60:40 mixture of ethylene glycol and water has an exponential dependence with temperature, namely:

$$\log(\mu_{nf}) = A\exp(-BT), \tag{17}$$

where the coefficients A and B are function of ϕ.

Khanafer and Vafai [165], instead, analyzed the viscosity of Al_2O_3–water nanofluids from the experimental data available in the literature [69,198,230,231]. The following empirical correlation was proposed as best fitting of literature results:

$$\mu_{nf} = -0.4491 + \frac{28.837}{T} + 0.574\phi - 0.1634\phi^2 + \frac{23.053\phi^2}{T^2} + 0.0132\phi^3 - \frac{2354.735\phi}{T^3} + \frac{23.498\phi^2}{d_p^2} - \frac{3.0185\phi^3}{d_p^2}, \tag{18}$$

with $1\% \le \phi \le 9\%$, $20\ ^\circ\text{C} \le T \le 70\ ^\circ\text{C}$ and $13\ \text{nm} \le d_p \le 131\ \text{nm}$.

Rudyak and Krasnolutskii [219] numerically estimated the viscosity of suspensions of aluminum and lithium nanoparticles (d_p=2 nm, T=300 K) in liquid argon as a function of nanoparticle size and material. Results revealed that the viscosity of the nanofluid had a quadratic dependence on the volume concentration:

$$\mu_r = 1 + a_1\phi + a_2\phi^2, \tag{19}$$

where a_1=3.20 and a_2=25.38 for Li nanoparticles, whereas a_1=3.25 and a_2=13.06 for Al nanoparticles. Rudyak and Krasnolutskii also found that viscosity increases with decreasing nanoparticle size:

$$\mu_r = \mu_{r,B} + (5.25\phi + 40.94\phi^2)\exp(-0.208 d_p/d_{bf}), \tag{20}$$

where $\mu_{r,B}$ is calculated according to Batchelor's relation [232] in Eq. (24), with d_p=1–4 nm and ϕ = 0.1–0.12.

5.1.3. Theoretical models

Several theoretical models have been introduced to model the dependence of nanofluid viscosity with the fluid characteristics and parameters [200,201,232–239].

First, the Einstein model [200] for infinitely dilute suspensions ($\phi \le 0.02$) containing spherical particles is formulated as:

$$\mu_r = \frac{\mu_{nf}}{\mu_{bf}} = (1 + 2.5\phi), \tag{21}$$

with μ_r being the enhanced viscosity ratio, μ_{bf} and μ_{nf} the effective viscosity of base fluid and nanofluid, respectively.

Brinkman [233] extended Einstein model to larger volume concentrations ($\phi < 0.04$):

$$\mu_r = \frac{\mu_{nf}}{\mu_{bf}} = \frac{1}{(1-\phi)^{2.5}} = 1 + 2.5\phi + 4.375\phi^2 + \ldots. \tag{22}$$

Lundgren [234] generalized Brinkman's method by proposing a Taylor series expansion, which is valid for the case of spherical particles suspensions and $\phi < 0.35$:

$$\mu_r = \frac{1}{1-2.5\phi} = 1 + 2.5\phi + 6.25\phi^2 + \ldots. \tag{23}$$

At low volume fractions, the second (or higher) orders of ϕ become negligible; therefore, Lundgren's model reduces to Einstein's model. Furthermore, Batchelor [232] considered the effect of both hydrodynamic interactions and Brownian motion of particles on the viscosity of homogeneous suspensions of spherical particles, and a relation similar to Lundgren's model has been obtained:

$$\mu_r = 1 + 2.5\phi + 6.2\phi^2. \tag{24}$$

Frankel and Acrivos [235], instead, related the viscous dissipation of energy in highly concentrated suspensions to the flow of a fluid within the narrow gaps between contiguous particles. As a result, the following expression has been obtained:

$$\mu_r = \frac{9}{8}\left[\frac{(\phi/\phi_m)^{\frac{1}{3}}}{1-(\phi/\phi_m)^{\frac{1}{3}}}\right], \tag{25}$$

where ϕ_m is the maximum attainable concentration, as experimentally determined. Graham [238] improved the work of Frankel and Acrivos by means of a cell theory approach. The obtained model considers two contributions to the energy dissipation rate in a fluid cell, namely a contribute due to neighbor particle interactions and a contribute due to the flow through the cell and around the reference sphere. These considerations lead to:

$$\mu_r = 1 + 2.5\phi + 4.5\left[\frac{1}{\left(\frac{h}{d_p}\right)\left(2+\frac{h}{d_p}\right)\left(1+\frac{h}{d_p}\right)^2}\right], \tag{26}$$

where h is the envelope interparticle distance and d_p the particle diameter.

Finally, theoretical models of nanofluid viscosity may also account for particle aggregation [201,236,240].

5.2. Density

The effective nanofluid density (ρ_{nf}) is usually evaluated by a mixing rule [69,195]:

$$\rho_{nf} = \frac{m_{nf}}{V_{nf}} = \frac{\rho_{bf}V_{bf} + \rho_p V_p}{V_{bf} + V_p} = (1-\phi)\rho_{bf} + \phi\rho_p, \tag{27}$$

where m_{nf} is the nanofluid mass, V_{nf} the nanofluid volume, V_{bf} the base fluid volume, V_p the particle volume and ρ_p the particle density. Pak et al. [69] and Ho et al. [195] noticed a good agreement between this relation and their experimental tests on alumina–water nanofluids.

The effect of temperature on nanofluid density is not considered in Eq. (27). Accurate fittings of experimental measures of ρ_{bf} at different temperatures [135,165,241,242] are usually obtained by [243]:

$$\rho_{bf} = \frac{a_0 + a_1 T + a_2 T^2 + a_3 T^3 + a_4 T^4 + a_5 T^5}{1 + a_6 T}, \tag{28}$$

where T is the temperature (°C) and a_0–a_6 are coefficients experimentally evaluated for the intended base fluid [242,243]. Considering Eqs. (28) and (27), Servati et al. [242] proposed a correlation for Al_2O_3–water nanofluids:

$$\rho_{nf} = \left(\frac{999.84 + 18.23T - 6.5\times10^{-3}T^2 - 5.4\times10^{-5}T^3}{0.0182T+1}\right) \times (1 - 1.1611\phi + 0.1611\phi^2) + \rho_p\phi(1-0.1611\phi), \tag{29}$$

in good agreement with experiments [195].

Also starting from the experimental results by Ho and colleagues [195], Khanafer and Vafai [165] presented a correlation between temperature and density of alumina–water nanofluids:

$$\rho_{nf} = (1001.064 + 2738.6191\phi - 0.2095T), \tag{30}$$

which is valid for $0 \le \phi \le 0.04$ and $5\ ^\circ\text{C} \le T \le 40\ ^\circ\text{C}$.

Finally, Vajjha et al. [241] measured the density of nanofluids containing alumina, antimony-tin oxide or zinc oxide nanoparticles suspended in a 60:40 (by weight) EG–water base fluid. To model the dependence of nanofluid density on temperature, Vajjha et al. took advantage of Eq. (27), assumed a constant value for ρ_p and considered:

$$\rho_{bf} = AT^2 + BT + C, \tag{31}$$

where $A = -2.43\times10^{-6}$ g/cm^3 K^2, $B = 9.6216\times10^{-4}$ g/cm^3 K and $C = 1.0099261$ g/cm^3.

Extended reviews regarding typical nanofluids densities can be found in references [69,192,195,241].

6. Nanofluids in automotive cooling systems

Some peculiar characteristics are required for coolants in automotive applications. Regarding the thermo-physical properties, a coolant should possess high thermal conductivity, specific heat capacity and boiling point, as well as low viscosity and freezing point. In addition, it should be non-toxic and chemically inert, and it should not cause corrosion of the cooling system. Commercially available coolants for automobiles are usually characterized by a 50:50 (by mass) mixture of ethylene glycol and water. Freezing and boiling points of this mixture are -34 °C and 107 °C, respectively [244]. However, typical engine coolants have low thermal conductivity, namely: 0.613 W/mK and 0.253 W/mK for water and EG at 27 °C, respectively (Table 2).

To enhance the heat transfer performance of cooling systems, it would be appropriate to use coolants with higher thermal conductivity. To this purpose, nanofluids can be an excellent alternative to traditional engine coolants, as evident from the typical thermal conductivity values in Table 3. On the other hand, regardless of the enhancement in thermal conductivity, viscosity and specific heat capacity may cast doubts on the application of nanofluids as coolants for automotive engines. Therefore, a critical investigation on the overall properties of nanofluids and their influence on the performance of the cooling circuit is necessary.

A brief study of the engine cooling circuit is performed in this section, followed by the evaluation of thermal performance and efficiency of prototype cooling systems running with nanofluids.

6.1. Engine cooling circuit

A typical engine cooling system consists of radiator, fan, water pump, coolant reservoir, thermostat and the necessary plumbing for both radiator and heater core. During the warming-up process, once the engine is started, the coolant is pumped from the lower radiator tank to the engine block, where the coolant is heated by engine cylinders. Thermostat does not open until the coolant reaches the operating temperature. The state at which coolant has reached the operating temperature is referred to as fully warmed-up condition. Then, heat energy is dissipated in the radiator, where heat is transferred to air flowing through the space between flat tubes and fins [25]. Usual temperature for the coolant at operating conditions is about 90 °C. The fan increases the heat transfer rate in the radiator in case of overheating. Moreover, the thermal energy accumulated in the coolant can be also used to heat up the cabin, thanks to an additional heater core.

It is highly beneficial to reduce warming-up time, as carbon monoxide (CO) and hydrocarbon (HC) emissions are much larger than in the fully warmed-up state (about 90% of HC emissions are

emitted in the first 20 s) [26]. Nanofluids may represent a way to decrease warming-up time. Let us consider an alumina-(W+EG) nanofluid: the effective specific heat capacity of the suspension is lower than the base fluid, while the density is higher. Hence, a lower volumetric heat capacity of nanofluid with respect to base fluid one means a faster warm-up phase, leading to better combustion efficiency as well as reduced CO and HC emissions.

The ϵ-NTU method is usually adopted to determine heat transfer rate and outlet temperature of coolants flowing through heat exchangers. Here, the typical design of automotive radiators is illustrated for both air and coolant sides, in order to highlight the possible effects of nanofluid coolants on thermal control systems in the automotive field.

The mass flow rate of air through the radiator ($\dot{m}_a$) can be evaluated as:

$$\dot{m}_a = \rho_a A_{c,a} u_a, \tag{32}$$

where ρ_a is the air density, $A_{c,a}$ the free flow area in the air side of radiator and u_a the air velocity. The convective heat transfer coefficient of air side (h_a) is instead evaluated as:

$$h_a = \frac{j_a \rho_a u_a c_{p,a}}{Pr^{2/3}}, \tag{33}$$

where j_a is the Colburn factor, $c_{p,a}$ the specific heat capacity of air and Pr the Prandtl number.

The efficiency of the fins in the radiator (η_{fin}) can be calculated as:

$$\eta_{fin} = \frac{\tanh(mL_{fin})}{mL_{fin}}, \tag{34}$$

where L_{fin} is the fin length and

$$m = \sqrt{\frac{2h_a}{k_{fin} t}}, \tag{35}$$

k_{fin} and t being the thermal conductivity and the thickness of fins, respectively. Note that, low fin length or thermal conductivity will result in lower fin efficiency. To account for the overall heat transfer efficiency of the radiator on the air side, the total surface effectiveness (η_0) is defined as [2,245]:

$$\eta_0 = 1 - (1 - \eta_{fin}) A_{ft}, \tag{36}$$

where A_{ft} is the ratio between fin area (A_{fin}) and total heat transfer surface (A).

Analogously, the mass flow rate of coolant ($\dot{m}_{nf}$) can be calculated as:

$$\dot{m}_{nf} = \rho_{nf} A_{c,nf} u_{nf}, \tag{37}$$

where $A_{c,nf}$ is the free flow area in the coolant side of radiator and u_{nf} the nanofluid velocity. The convective heat transfer coefficient of coolant side (h_{nf}) can be evaluated as:

$$h_{nf} = \frac{Nu_{nf} k_{nf}}{D_{h,nf}}, \tag{38}$$

where Nu_{nf} is the Nusselt number of the coolant (e.g. nanofluid), which depends on both characteristics of the system [9,25,246] and hydraulic diameter of the radiator tube ($D_{h,nf}$).

By neglecting the tube-wall thermal resistance, the overall heat transfer coefficient of the radiator (U_r) can be evaluated as:

$$\frac{1}{U_r} = \frac{1}{\eta_0 h_a} + \frac{1}{\frac{\alpha_{nf}}{\alpha_a} h_{nf}}, \tag{39}$$

where α_a and α_{nf} are the ratio between total heat transfer area and total radiator volume (V_r) for air and nanofluid sides, respectively.

The ϵ-NTU method can be then adopted, where the number of heat transfer units (NTU) is:

$$NTU = \frac{U_a \alpha_a V_r}{C_{min}}, \tag{40}$$

with $C_{min} = \min(C_a, C_{nf})$ being the minimum heat capacity rate between air and nanofluid. Heat capacity rate for air or nanofluid can be calculated as:

$$C = \dot{m} c_p. \tag{41}$$

The capacity ratio (C^*) between air and nanofluid is:

$$C^* = \frac{C_{min}}{C_{max}}, \tag{42}$$

where $C_{max} = \max(C_a, C_{nf})$. Subsequently, the heat exchanger effectiveness (ϵ) for a pure unmixed cross-flow configuration with an infinite number of passages is found as [245]:

$$\epsilon = 1 - \exp\left(\frac{1}{C^*}\right) (NTU)^{0.22} \left[\exp[-C^* (NTU)^{0.78}] - 1\right]. \tag{43}$$

The heat flux exchanged in the radiator ($\dot{Q}$) can be finally evaluated as:

$$\dot{Q} = \epsilon C_{min} (T_{nf,in} - T_{a,in}), \tag{44}$$

where $T_{nf,in}$ and $T_{a,in}$ are the inlet temperature of coolant and air, respectively.

The pressure drop experienced by the coolant in the radiator (ΔP_{nf}) can be estimated as:

$$\Delta P_{nf} = \frac{f_{nf} L_r \rho_{nf} u_{nf}^2}{2 D_{h,nf}}, \tag{45}$$

where f_{nf} is the friction factor of nanofluid coolant [9,25] and L_r the radiator length. Eventually, the required pumping power (W) is:

$$W = \dot{V}_{nf} \Delta P_{nf}, \tag{46}$$

where $\dot{V}_{nf}$ is the nanofluid volumetric flow rate.

6.2. Efficiency of nanofluid coolants

The heat transfer enhancement by nanofluid coolants is generally accompanied with the increase in pressure drop [247]. Hence, a compromise between the higher heat transfer and the associated higher pressure losses has to be considered by introducing performance indexes.

In a experimental study, Razi et al. [248] investigated the heat transfer and pressure drop characteristics of the flow of a nanofluid in a tube. To improve the heat transfer coefficient, they adopted nanofluid coolants (i.e. CuO–oil) and flattened tubes, instead of conventional base fluids and round tubes. Then, heat transfer coefficient and pressure drop were measured in a broad variety of configurations. To quantify the overall benefits of nanofluid coolants, they defined an efficiency coefficient as:

$$\eta_I = \frac{\left(\frac{h^*}{h_{RT,bf}}\right)}{\left(\frac{\Delta P^*}{\Delta P_{RT,bf}}\right)}. \tag{47}$$

h^* and ΔP^* are heat transfer coefficient and pressure drop for the nanofluid configuration, respectively, whereas $h_{RT,bf}$ and $\Delta P_{RT,bf}$ refer to the flow of conventional oil coolant inside a round tube. Based on Eq. (47), a performance index (η_I) greater than 1 implies that the advantages due to heat transfer enhancement by either nanofluid or flattened tubes overcome the increase in pressure drop. In particular, Razi et al. [248] found that a maximum value for the performance index (i.e. $\eta_I = 1.43$) was observed for the nanofluid flow within flattened tubes with an internal height of

7.5 mm and $Re=23.5$. Specifically, they found that:

$$\eta_{I,nf,FT} > \eta_{I,nf,RT} > \eta_{I,bf,RT},$$

which indicates that using nanofluids within flat tubes is an efficient strategy for enhancing overall performances of traditional heat exchangers.

Results from Razi et al. [248] experiments also showed that the Nusselt number for the CuO–oil nanofluid (<2 wt% particle concentration) in the fully developed hydrodynamic laminar flow regime ($Re<120$) and within flattened tubes ($1<D/D_h<1.3$) can be interpolated by:

$$Nu_{nf}=0.0812Re_{nf}^{0.587}Pr_{nf}^{0.389}\left(\frac{D}{D_h}\right)^{1.297}(1+\phi)^{56.147}, \quad (48)$$

where Re_{nf} is the nanofluid Reynolds number, Pr_{nf} the nanofluid Prandtl number, D the round tube diameter, and D_h the flattened tube hydraulic diameter. Hence, the heat transfer coefficient was finally calculated as:

$$h_{nf}=\frac{Nu_{nf}\times k_{nf}}{D^*}, \quad (49)$$

where D^* stands for either D or D_h.

On the other hand, Ray at al. [25] suggested to calculate Nu of the base fluid inside flat tubes with the Bejan and Gnielinski correlations [249,250]:

$$Nu_{bf}=0.012(Re_{bf}^{0.87}-280)Pr_{bf}^{0.4}, \quad (50)$$

with $1.5\le Pr_{bf}\le 500$ and $3\times 10^3\le Re_{bf}\le 10^6$. Instead, they proposed an expression derived by Vajjha et al. [251] to compute Nu of the nanofluid coolant:

$$Nu_{nf}=0.0222(Re_{nf}^{0.8}-60)Pr_{nf}^{0.4}(1+0.32178\phi^{0.64788}), \quad (51)$$

with $17.6\le Pr_{nf}\le 38.6$ and $3000\le Re_{nf}\le 16,000$.

Ferrouillat and co-workers [252] carried out an experimental work on the influence of nanoparticle shape on the overall energy performances of nanofluids for cooling applications. They measured the pressure drops and heat transfer coefficients of water-based SiO_2 and ZnO nanofluids, which were flowing within a horizontal tube at different inlet temperatures and flow rates. Results indicated a small improvement in the Nusselt number with nanofluid coolants. Moreover, they defined a second efficiency coefficient (η_{II}) to characterize the performance of fluid coolants. This coefficient compares the heat flux transferred ($\dot{Q}$) and the required pumping power (W) for nanofluid and conventional coolants, namely:

$$\eta_{II}=\frac{\dot{Q}_{nf}/W_{nf}}{\dot{Q}_{bf}/W_{bf}}, \quad (52)$$

where $\dot{Q}$ and W are derived from Eqs. (44) and (46), respectively. Results showed that $\eta_{II}>1$, i.e. nanofluid coolants with overall energy performances higher than water, only in case of suspended ZnO nanoparticles with shape factor greater than 3.

6.3. Nanofluid coolants for automotive applications

Taking advantage from the relations between nanofluid characteristics and resulting thermo-physical properties discussed in previous sections, it may be possible to rationally design nanofluids with large heat transfer rate while keeping the required pumping power as low as possible. In the following, some of the research works on the application of nanofluids in automotive radiators are reviewed.

In a numerical study, Bai et al. [253] assessed the heat transfer capability of Cu, Al, Al_2O_3 and TiO_2 water-based nanofluids in an engine cooling system ($\dot{V}=155$ l/min). According to their results, the Cu–water nanofluid ($\phi=5\%$) showed the largest heat transfer coefficient ($h_{nf}=6251.77$ W/m^2 K), namely 46% more than pure water ($h_{bf}=4282.84$ W/m^2 K). Hence, the average heat dissipation potential of the nanofluid for a single cylinder ($\dot{Q}=2937.2$ W) was 43.9% higher than in case of pure water. The pumping power, instead, increased by 6% because of the higher pressure drop for Cu–water nanofluid ($\Delta P_{nf}=24$ kPa) as compared to water coolant ($\Delta P_{bf}=17$ kPa).

Vajjha et al. [168] performed a numerical study for assessing both fluid dynamics and heat transfer performance of Al_2O_3 and CuO nanofluids in the flat tubes of a radiator. The nanofluid flow was under laminar regime, with Reynolds numbers spanning from 100 to 2000. Results allowed establishing two new correlations for the Nusselt number in the entrance region:

$$Nu=1.9421\left(RePr\frac{D_h}{Z}\right)^{0.3}, \quad (53)$$

valid for

$$\left(RePr\frac{D_h}{Z}\right)\ge 33.33,$$

and

$$Nu=6.1+0.003675\left(RePr\frac{D_h}{Z}\right), \quad (54)$$

valid for

$$\left(RePr\frac{D_h}{Z}\right)<33.33,$$

where Z is the axial distance from the inlet. This analysis showed a heat transfer increase with both Reynolds number and particle concentration. Based on their numerical results, heat transfer coefficients of Al_2O_3 ($\phi=10\%$) and CuO ($\phi=6\%$) nanofluids at $Re=2000$ were 94% and 89% higher than the base fluid, respectively. Furthermore, they observed that, for a constant inlet velocity, the friction factor along the duct increased with the particle volume concentration. On the other hand, the same heat transfer coefficient could be achieved by a lower volumetric flow rate of nanofluids than conventional coolants, and thus less pumping power was required. In fact, in the laminar flow regime and for the same amount of heat transferred, the required pumping power for Al_2O_3 ($\phi=10\%$) and CuO nanofluids ($\phi=6\%$) was 82% and 77% lower than the one required for the base fluid, respectively. Hence, the performance index (η_I) was 1.30 and 1.14 for the alumina and copper oxide nanofluids, respectively ($Re=2000$ and $h=910$ W/m^2 K). These results are a preliminary proof of the potential of using nanofluid coolants in car radiators.

Peyghambarzadeh et al. [254] experimentally analyzed the heat transfer performance of a nanofluid in a car radiator with louvered fins and flat tubes. They carried out a systematic experimental evaluation of the thermal transfer efficiency with pure water, pure ethylene glycol (EG) as well as water–EG mixtures. Subsequently, Al_2O_3 nanoparticles were added in these base fluids, and the resulting performance variations recorded (particle volume concentration spanning from 0.1 to 1%; flow rate from 1 to 6 l/min). The Nusselt number in the nanofluid cases increased up to 40% with both volume concentration of particles and Reynolds number. Furthermore, Peyghambarzadeh and colleagues found that by increasing the nanofluid inlet temperature ($T_{nf,in}$) from 35 °C to 50 °C, the Nusselt number of water-based nanofluids increased by 16%. Instead, for the EG-based nanofluids, an enhancement of 7% was evident by increasing the $T_{nf,in}$ from 45 °C to 60 °C. Eventually, they also studied the performance of EG- and water-based alumina nanofluids by varying the concentration of EG (from 5% to 20%), the Al_2O_3 volume concentration (from 0 to 0.3%) and the flow rate. Results showed that by increasing the EG percentage in water, the Nusselt number decreased, since water has better thermal

properties than EG. Moreover, by increasing the particle volume fraction and flow rate, the Nusselt number significantly increased.

Hussein et al. [24] performed an experimental and computational study of the heat transfer performances of a car radiator running with SiO_2–water nanofluid under laminar flow. They set up a test rig to measure heat transfer coefficient and friction factor of the nanofluid coolant (Fig. 7). Hussein and colleagues observed that the friction factor of nanofluid was inversely proportional to the flow rate, whereas directly proportional to the particle volume fraction. The decrease in friction factor by increasing the Reynolds number, instead, was in accordance with the Darcy–Weisbach equation for laminar flow conditions. Moreover, the Nusselt number increased with flow rate, nanofluid volume concentration and inlet temperature. Particularly, the increase of inlet temperature ($T_{nf,in}$) from 60 °C to 80 °C led to Nusselt number increase from 17.8 to 25. Therefore, SiO_2–water nanofluids with low volume concentration of nanoparticles were proven to be able to enhance heat transfer rate up to 50% compared to pure water.

Leong et al. [9] investigated the heat transfer characteristics of EG-based copper nanofluids in a car radiator. They observed that, at a fixed air side Reynolds number (i.e. $Re=4000$), the overall heat transfer coefficient on the air side increased with both Reynolds number of coolant and volume concentration of particles (Fig. 8). Hence, they concluded that the use of nanofluids may allow reducing the heat transfer area of automotive radiators. A reduction of 18.7% was estimated for the air frontal area at $Re_{air}=6000$ and $Re_{coolant}=5000$ when the base fluid was replaced by a 2% copper nanoparticle suspension. Furthermore, Leong et al. noticed an increase in coolant pressure drop with the addition of copper nanoparticles. Results revealed a pressure drop of 110.97 kPa by adding 2% copper particles, instead of 98.93 kPa in case of pure water. Hence, an additional pumping power of 12.13% was required with nanofluid coolants at 0.2 m^3/s volumetric flow rate. Considering the data available in this study at $Re_{air}=4000$ and $Re_{coolant}=7000$, the energy efficiency of the 2% Cu–EG nanofluid coolant $\eta_I \approx 1$ in Eq. (47) was found, meaning that no significant overall performance improvement in using nanofluid rather than traditional coolants was noticed.

Huminic et al. [255] employed a numerical approach to assess the heat transfer characteristics of a CuO–EG nanofluid flowing in flattened tubes of automobile radiator under a laminar flow regime. They evaluated the effects of volume concentration (0–4%) and Reynolds number (0–125) on the heat transfer performance of the car radiator. Results showed a *Nu* increase with both volume fraction and Reynolds number. For instance, a 19% enhancement in the heat transfer coefficient at $Re=10$ and $\phi=4\%$ was reported. Furthermore, by comparing flattened, elliptical and circular tubes, they realized that flattened tubes can substantially increase (up to 82% enhancement, Fig. 9) heat transfer coefficient.

In summary, thermo-physical properties of nanofluids (ρ, μ, c_p, k) have been observed to change with nanofluid characteristics (e.g. particle volume fraction, particle shape and size, particle and base fluid material, and temperature). The variation of the nanofluid characteristics, on one hand, leads to changes in the

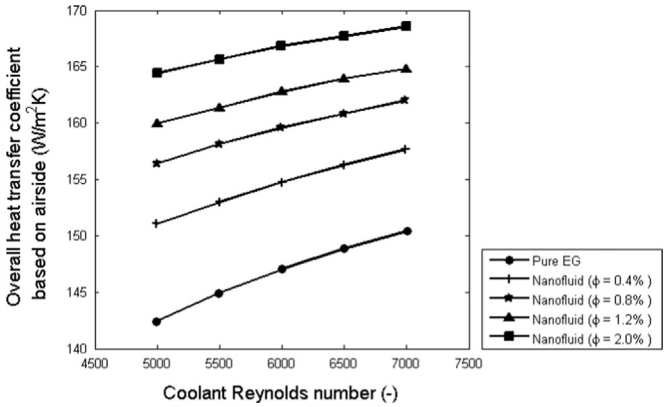

Fig. 8. Air side overall heat transfer coefficient of Cu–EG nanofluids at different Reynolds numbers and particle volume fraction. Figure reproduced based on reference [9].

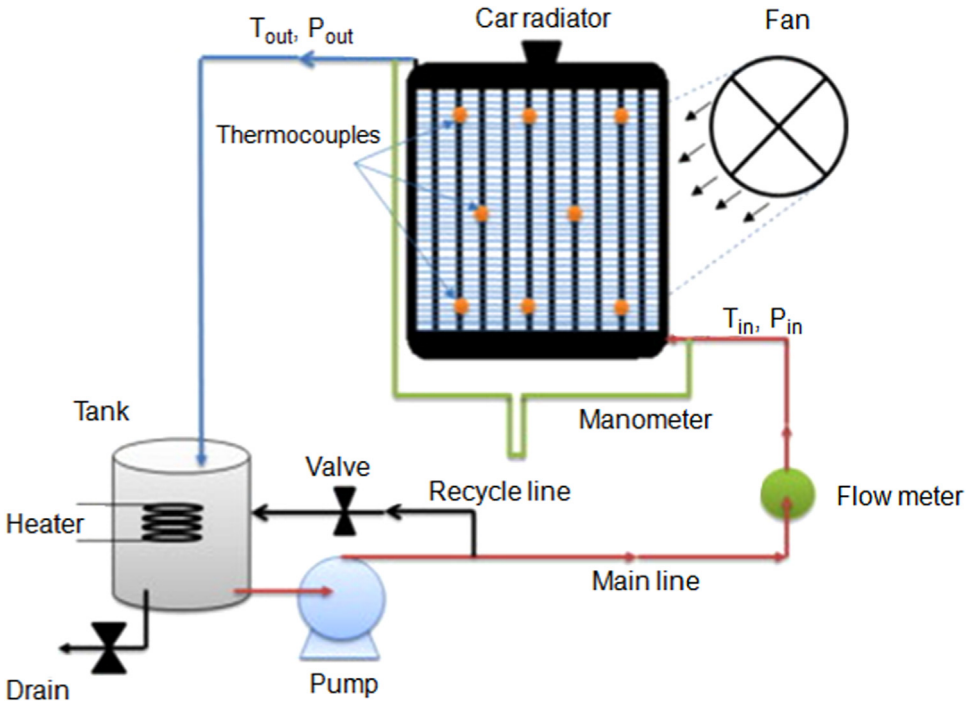

Fig. 7. Schematic diagram of an experimental test rig for nanofluid coolants. The test rig includes an automotive radiator, 10 thermocouples type T to measure temperature, tubes (0.5 in), a fan, a manometer tube with mercury, a flow meter , two valves, a centrifugal pump (0.5 hp and 3 m head), a reservoir plastic tank, a DC power supply and an electrical heater. Figure adopted from reference [24].

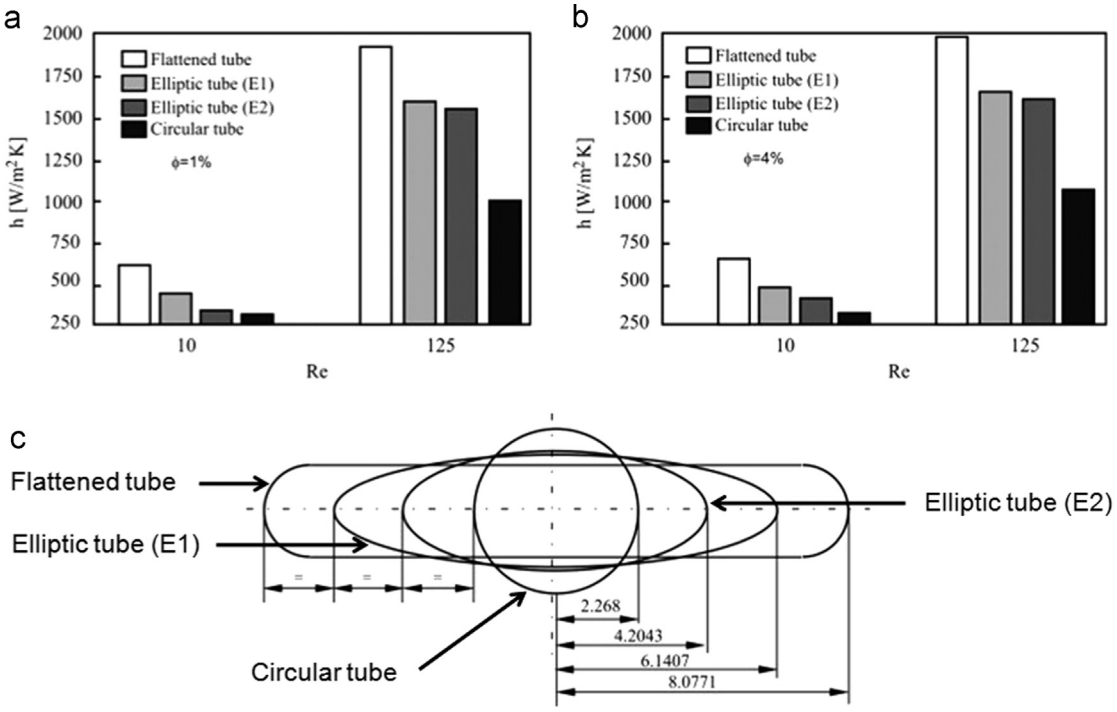

Fig. 9. Heat transfer coefficient of a radiator tube. (a) Influence of *Re* and tube cross section on h_{nf} at $\phi = 1\%$ (b) Influence of *Re* and tube cross section on h_{nf} at $\phi = 4\%$ (c) Considered tube cross sections. Figure adopted from reference [255].

dimensionless numbers (i.e. *Re* and *Pr*) required for evaluating the heat transfer coefficient of cooling system. On the other hand, the variation in *Re* leads to changes in *f*, ΔP and hence the required pumping power, which is generally higher for systems working with nanofluid coolants. Hence, one should systematically assess the overall influence of these parameters on the energy performance of the system by means of the efficiency indexes in Eqs. (47) and (52).

7. Challenges and perspectives

In this section, the challenges and barriers to a wider industrial application of nanofluids are reviewed. Moreover, perspectives for a further development of nanofluid research are indicated, with the aim to resolve the inconsistencies reported in the current literature.

First, properties of nanofluids cannot be predicted by classical continuum models and, currently, there is no general theoretical model which can forecast their heat and mass transfer characteristics. Particularly, several mechanisms have been proposed to explain the enhanced heat conduction of nanofluids, such as nanolayer, interfacial thermal resistance, aggregation and percolation phenomena. However, the interplay between these mechanisms and the resulting effect on thermo-physical properties of nanofluids have not yet been systematically understood. Second, evidences from different experimental studies are not consistent, and usually not even well understood. Third, large-scale and low-cost production of stable nanoparticle suspensions has not yet been achieved.

Various geometrical, chemical and physical parameters can affect the nanofluid stability, as well as its heat transfer and rheological properties. Hence, a possible explanation for the existence of contradictory experimental results could be the different production techniques and experimental protocols adopted for synthesizing and testing nanofluids. These inconsistencies strongly influence the nanofluid properties.

To address these controversies and allow a more systematic study of the underlying physical phenomena, experimental studies on nanofluids should always detail: (1) the synthesis method adopted for preparing the nanofluid; (2) the nanoparticle characteristics (core and coating material, particle shape) as well as the type of surfactant introduced (if any); (3) the concentration of nanoparticles and surfactants; (4) the size distribution of nanoparticles; (5) the base fluid properties; (6) the pH and zeta-potential of the suspension during different stages of the experiment; (7) the concentration of additives used for adjusting the pH of the suspension (if any); (8) the presence of particle clusters as well as the average aggregates size; (9) the time elapsed after the nanofluid synthesis; (10) the temperature at which experiments are conducted; and (11) the measurement techniques adopted and any other helpful data that can provide the reader with a complete understanding of the conducted experiment.

On the other hand, results of experimental studies on nanofluids should be properly analyzed. It is generally accepted that by suspending nanoparticles in a base fluid, effective thermal conductivity, viscosity and density increase, while heat capacity decreases. Hence, the nanofluid performance cannot be judged by merely evaluating the resulting heat transfer coefficient (h_{nf}), while an overall analysis should be considered. In particular, a meaningful quantity to assess the technical feasibility of nanofluids as automotive coolants is the efficiency index, which compares the beneficial enhancement in thermal conductivity with the general viscosity (i.e. pumping power) increase. Similarly, also the Prandtl number is a good reference for evaluating the balance between thermal conductivity and viscosity enhancements in nanofluids. As reported in Tables 4 and 5, the calculated efficiencies and Prandtl numbers for several studies are larger than one, therefore demonstrating that nanofluids are energy efficient alternatives to traditional automotive coolants. In addition, the working conditions of the nanofluid in each specific application should be critically investigated. Considering typical automotive cooling system, the operating conditions of the engine and thus of the cooling circuit, such as temperature, flow regime and the

suitable coolant pH, should be taken into account. Engine coolants usually operate in the temperature range between 50 °C and 110 °C [25]. In that temperature interval, nanofluid thermal conductivity tends to increase with temperature, while viscosity decreases. However, there exists a critical temperature beyond which a irreversible degradation of nanofluid properties may occur.

Another important factor influencing the performances of nanofluid coolants is the flow regime, which can drastically change their thermal and rheological properties. Moreover, the pH of coolant should be carefully designed, since it has direct impact on the corrosion of radiator and tubes in automotive cooling systems [244]: for most of the cars, pH should be maintained in the range 7.5–10.5 [257]. Hence, the pH of nanofluids can be adjusted towards these practical range, which also induces further thermal conductivity enhancements (Table 6). Considering the zeta-potential and the pH range in Table 6, one can understand that those thermal conductivity enhancements have been reported far from the isoelectric points of Al_2O_3–water and Cu–water suspensions. For this reason, the thermal conductivity enhancement and viscosity variation in nanofluid coolants should be generally convenient within the practical pH range for automotive applications.

Finally, the development of large-scale production techniques is also required to obtain nanofluids with good stability, repeatability and low production costs. Both the current single- and two-step techniques are facing difficulties that should be addressed to scale up nanofluids synthesis. As regards two-step methods, the challenge is to overcome large van der Waals agglomeration of nanoparticles, for example by means of proper surface treatment or particle coating. The current drawbacks of single-step techniques, instead, are the higher cost of synthesis, as well as the limited control over nanoparticle size distribution.

Table 4
Energy efficiency of nanofluids for automotive cooling applications.

NP material	Base fluid	ϕ (%)	T (°C)	η_I	η_{II}	Reference
Cu	W	5	70	1.034	1.019	[253]
CuO	60:40 EG/W	6	90	1.141	–	[168]
Al_2O_3	60:40 EG/W	10	90	1.304	–	[168]
CuO	Oil	2 (wt%)	–	1.43	–	[248]
ZnO	W	0.93	15–90	–	1.097	[252]
SiO_2	W	2.28	15–90	–	0.930	[252]

Table 5
Prandtl number enhancement in nanofluids for automotive cooling applications.

NP material	Base fluid	ϕ (%)	T (°C)	Pr_{nf}/Pr_{bf}	References
Al_2O_3	60:40 EG/W	5	25	1.475	[25]
CuO	60:40 EG/W	5	25	2.064	[25]
SiO_2	60:40 EG/W	5	25	1.231	[25]
Cu	W	2	70	0.914	[253]
Al	W	2	70	0.916	[253]
TiO_2	W	2	70	0.939	[253]
SiO_2	W	2	50	0.867	[24,256]
Al_2O_3	W	2	50	1.605	[24,256]
TiO_2	W	2	50	1.379	[24,256]
Al_2O_3	W	1	77	0.953	[26]

8. Conclusions

Thanks to their enhanced thermo-physical properties, nanofluids are showing great potential in energy, mechanical and biomedical fields. Mainly, the high thermal conductivity of nanofluids can guarantee extremely efficient heat exchange in automotive cooling applications. However, a more rational design of these nanoparticle suspensions requires a better understanding of their nanoscale characteristics and resulting macroscale properties. This review supplies an in-depth description of the state of the art in nanofluids, from the synthesis to their thermo-physical properties, in the context of automotive applications.

Special attention is paid to the critical dependency of thermal conductivity (k_{nf}) on nanoscale mechanisms in nanofluids. In detail, k_{nf} is strongly enhanced by a highly conductive liquid nanolayer around the surface of the particles. Moreover, particle–fluid heat conduction is also affected by the interfacial thermal resistance, which is not negligible at this scale. Brownian motion also plays a crucial role in nanofluid properties: although particle diffusion is extremely slow compared to heat diffusivity, Brownian motion affects the agglomeration of particles and thus the formation of thermal percolating paths. Unfortunately, significant aggregation into sparse but large clusters increases both thermal transport and fluid viscosity. Hence, future researches should investigate the optimal nanofluid aggregate morphologies leading to the best combination of thermal conductivity, viscosity and stability.

This review presents several theoretical and empirical models describing nanofluid thermal conductivity, viscosity, specific heat capacity and density. Specifically, a strong sensitivity of nanofluid properties to their design characteristics (i.e. particle material, shape, size and volume concentration, base fluid pH and surfactant concentration) is noticeable in the available literature. This extremely pronounced sensitivity could be identified as the main reason for some contradictory results in the large amount of models and the experimental evidences in the literature.

The ultimate purpose of this review is highlighting the advantages of nanofluids as coolants for automotive heat exchangers, and a number of guidelines have been suggested for their rational design and usage. However, although thousands of studies have addressed a more mechanistic understanding of nanofluid properties, comprehensive models relating nanoscale effects to their macroscopic behavior are still missing. Such multiscale models would facilitate and systematize the translation of nanofluid technology from small-scale experiments to large scale industrial production and commercialization.

Table 6
Nanofluid properties at practical pH ranges for automotive applications.

Nanofluid	pH range	Zeta potential (mV)	Weight fraction	k_{nf}/k_{bf}	Temperature (°C)	Surfactant	References
Cu–water	8–11	−44 to −40	0.05 (wt%)	9 %	25	SDBS	[77,118]
Al_2O_3–water	8–11	−40 to −33	0.05 (wt%)	8 %	25	SDBS	[118]
ZrO_2–water	8–10	−12 to −25	3 (wt%)	5–30 %	25	–	[136]
TiO_2–water	–	−47.9	0.1 (wt%)	10 %	–	SDS	[258]

Acknowledgments

Authors would like to acknowledge the NANO-BRIDGE – Heat and mass transport in NANO-structures by molecular dynamics, systematic model reduction, and non-equilibrium thermodynamics (PRIN 2012, Grant number 2012LHPSJC) – the NANO-STEP – NANOfluid-based direct Solar absorption for Thermal Energy and water Purification (Fondazione CRT, Torino) projects and the DRAPO projects. Authors are grateful to Gianmarco Ciorra for some supporting literature review.

References

[1] Wen D, Lin G, Vafaei S, Zhang K. Review of nanofluids for heat transfer applications. Particuology 2009;7(2):141–50.
[2] Webb RL, Kim N-H. Principal of enhanced heat transfer. New York, NY, USA: Taylor Francis; 1994.
[3] Liu S, Sakr M. A comprehensive review on passive heat transfer enhancements in pipe exchangers. Renew Sustain Energy Rev 2013;19:64–81.
[4] Cola F, Gennaro De M, Perocchio D, Canuto E, Daniele S, Napoli P, et al. Integrated receivers with bottom subcooling for automotive air conditioning: detailed experimental study of their filling capacity. Int J Refrig 2016;62:72–84, http://dx.doi.org/10.1016/j.ijrefrig.2015.08.021.
[5] Ventola L, Dialameh M, Fasano M, Chiavazzo E, Asinari P. Convective heat transfer enhancement by diamond shaped micro-protruded patterns for heat sinks: thermal fluid dynamic investigation and novel optimization methodology. Appl Therm Eng 2016;93:1254–63.
[6] Chiavazzo E, Ventola L, Calignano F, Manfredi D, Asinari P. A sensor for direct measurement of small convective heat fluxes: validation and application to micro-structured surfaces. Exp Therm Fluids Sci 2014;55:42–53.
[7] Ventola L, Robotti F, Dialameh M, Calignano F, Manfredi D, Chiavazzo E, et al. Rough surfaces with enhanced heat transfer for electronics cooling by direct metal laser sintering. Int J Heat Mass Transf 2014;75:58–74.
[8] Kulkarni DP, Vajjha RS, Das DK, Oliva D. Application of aluminum oxide nanofluids in diesel electric generator as jacket water coolant. Appl Therm Eng 2008;28(1415):1774–81.
[9] Leong K, Saidur R, Kazi S, Mamun A. Performance investigation of an automotive car radiator operated with nanofluid-based coolants (nanofluid as a coolant in a radiator). Appl Therm Eng 2010;30:2685–92.
[10] Hercamp RD, Hudgens RD, Coughenour GE. Aqueous propylene glycol coolant for heavy duty engines. Technical report. SAE technical paper; 1990.
[11] Boyle RJ, Finlay I, Biddulph T, Marshall R. Heat transfer to non-aqueous engine coolants. Technical report. SAE technical paper; 1991.
[12] Kilmartin WJ, Dehm DC. Aqueous propylene glycol engine coolant for automotive and light duty applications. Technical report. SAE technical paper; 1993.
[13] Zadrozny A. Propylene glycol coolant: a safer alternative for heavy duty vehicles. Technical report. SAE technical paper; 1993.
[14] Washington DA, Miller DL, Maes J-P, Van de Ven P, Orth JE. Long life performance of carboxylic acid based coolants. Technical report. SAE technical paper; 1994.
[15] Coughenour GE, Goodman DR, Brunett AJ, Ellis SL. High temperature, high load performance of propylene glycol engine coolants in modern gasoline engines. Technical report. SAE technical paper; 1995.
[16] Gollin M, McAssey EV, Stinson C. Comparative performance of ethylene glycol/water and propylene glycol/water coolants in the convective and forced flow boiling regimes. Technical report. SAE technical paper; 1995.
[17] Choi SU, Eastman J. Enhancing thermal conductivity of fluids with nanoparticles. Technical report. IL, United States: Argonne National Lab; 1995.
[18] Vanaki SM, Ganesan P, Mohammed H. Numerical study of convective heat transfer of nanofluids: a review. Renew Sustain Energy Rev 2016;54:1212–39.
[19] Chandrasekar M, Suresh S, Bose AC. Experimental studies on heat transfer and friction factor characteristics of Al_2O_3/water nanofluid in a circular pipe under laminar flow with wire coil inserts. Exp Therm Fluid Sci 2010;34(2):122–30.
[20] He F, Ewing D, Finn J, Wagner J, Ma L. Thermal management of vehicular payloads using nanofluid augmented coolant rail-modeling and analysis. Technical report. SAE technical paper; 2013.
[21] Saidur R, Leong K, Mohammad H. A review on applications and challenges of nanofluids. Renew Sustain Energy Rev 2011;15(3):1646–68.
[22] Corcione M, Cianfrini M, Quintino A. Optimization of laminar pipe flow using nanoparticle liquid suspensions for cooling applications. Appl Therm Eng 2013;50(1):857–67.
[23] Srivastava S, Chauhan NS. Nanofluids: effectual analysis in automotive application. Technical report. SAE technical paper; 2014.
[24] Hussein AM, Bakar R, Kadirgama K. Study of forced convection nanofluid heat transfer in the automotive cooling system. Case Stud Therm Eng 2014;2:50–61.
[25] Ray DR, Das DK. Superior performance of nanofluids in an automotive radiator. J Therm Sci Eng Appl 2014;6(4):041002.
[26] Millan MV, Samuel S. Nanofluids and Thermal Management Strategy for Automotive Application. Technical report. SAE technical paper; 2015.
[27] Amiri A, Shanebedi M, Chew B, Kazi S, Solangi K. Toward improved engine performance with crumpled nitrogen-doped graphene based water-ethylene glycol coolant. Chem Eng J 2016;289:583–95, http://dx.doi.org/10.1016/j.cej.2015.12.083.
[28] Borbáth T, Bica D, Potencz I, Vékás L, Borbáth I, Boros T. Magnetic nanofluids and magnetic composite fluids in rotating seal systems, in: IOP conference series: earth and environmental science, vol. 12. IOP Publishing; 2010. p. 012105, 25th IAHR Symposium on Hydraulic Machinery and Systems, Timisoara, Romania, 20–24 September 2010. http://dx.doi.org/10.1088/1755-1315/12/1/012105.
[29] Choi CJ, Jang SP, Choi SU. Electrokinetic effects of charged nanoparticles in microfluidic Couette flow. J Colloid Interface Sci 2011;363(1):59–63.
[30] Lee K, Hwang Y, Cheong S, Kwon L, Kim S, Lee J. Performance evaluation of nano-lubricants of fullerene nanoparticles in refrigeration mineral oil. Curr Appl Phys 2009;9(2 (Supplement)):e128–31.
[31] Moradi A, Sani E, Simonetti M, Francini F, Chiavazzo E, Asinari P. Carbon-nanohorn based nanofluids for a direct absorption solar collector for civil application. J Nanosci Nanotechnol 2015;15(5):3488–95.
[32] Zhang L, Ding Y, Povey M, York D. ZnO nanofluids—a potential antibacterial agent. Prog Nat Sci 2008;18(8):939–44.
[33] Liu J, Yan J-F, Deng Z-S. Nano-cryosurgery: a basic way to enhance freezing treatment of tumor. In: ASME 2007 international mechanical engineering congress and exposition; 2007. p. 87–94.
[34] Gizzatov A, Key J, Aryal S, Ananta J, Cervadoro A, Palange AL, et al. Hierarchically structured magnetic nanoconstructs with enhanced relaxivity and cooperative tumor accumulation. Adv Funct Mater 2014;24(29):4584–94.
[35] Cervadoro A, Cho M, Key J, Cooper C, Stigliano C, Aryal S, et al. Synthesis of multifunctional magnetic nanoflakes for magnetic resonance imaging, hyperthermia, and targeting. ACS Appl Mater Interfaces 2014;6(15):12939–46.
[36] Global I. Industry Analysts. Automotive radiators: a global strategic business report. ⟨http://www.strategyr.com/Automotive_Radiators_Market_Report.asp⟩; 2015.
[37] Choi S. Enhancing thermal conductivity of uids with nanoparticles. In: ASME-publications-Fed, vol. 231; 1995. p. 99–106.
[38] Keblinski P, Phillpot S, Choi S, Eastman J. Mechanisms of heat flow in suspensions of nano-sized particles (nanofluids). Int J Heat Mass Transf 2002;45(4):855–63.
[39] Murshed S, Leong K, Yang C. Enhanced thermal conductivity of TiO_2 water based nanofluids. Int J Therm Sci 2005;44(4):367–73.
[40] Xu J, Bandyopadhyay K, Jung D. Experimental investigation on the correlation between nano-fluid characteristics and thermal properties of Al_2O_3 nano-particles dispersed in ethylene glycol-water mixture. Int J Heat Mass Transf 2016;94:262–8.
[41] Azmi W, Sharma K, Mamat R, Najafi G, Mohamad M. The enhancement of effective thermal conductivity and effective dynamic viscosity of nanofluids—a review. Renew Sustain Energy Rev 2016;53:1046–58.
[42] Kakaç S, Pramuanjaroenkij A. Single-phase and two-phase treatments of convective heat transfer enhancement with nanofluids—a state-of-the-art review. Int J Therm Sci 2016;100:75–97.
[43] Celata GP, D'Annibale F, Mariani A, D'Amato RD, Bubbico R. Heat transfer in water-based SiC and TiO_2 nanofluids. Heat Transf Eng 2013;34(13):1060–72.
[44] Chiavazzo E, Asinari P. Enhancing surface heat transfer by carbon nanofins: towards an alternative to nanofluids? Nanoscale Res Lett 2011;6:249.
[45] Timofeeva EV, Yu W, France DM, Singh D, Routbort JL. Nanofluids for heat transfer: an engineering approach. Nanoscale Res Lett 2011;6(1):1–7.
[46] Wang X-Q, Mujumdar AS. A review on nanofluids-Part II: experiments and applications. Braz J Chem Eng 2008;25(4):631–48.
[47] Das S, Choi S, Yu W, Pradeep T. Nanofluids: science and technology. Hoboken, NJ (USA): Wiley; 2007 ISBN: 978-0-470-07473-2.
[48] Krajnik P, Pusavec F, Rashid A. Nanofluids: properties, applications and sustainability aspects in materials processing technologies. In: Advances in sustainable manufacturing. Springer; 2011. p. 107–13, Proceedings of the 8th Global Conference on Sustainable Manufacturing, Abu Dhabi, November 22 – 24, 2010. ISBN: 978-3-642-20182-0.
[49] Colla L, Marinelli L, Fedele L, Bobbo S, Manca O. Characterization and simulation of the heat transfer behaviour of water-based ZnO nanofluids. J Nanosci Nanotechnol 2015;15(5):3599–609.
[50] Ahammed N, Asirvatham LG, Titus J, Bose JR, Wongwises S. Measurement of thermal conductivity of graphene-water nanofluid at below and above ambient temperatures. Int Commun Heat Mass Transf 2016;70:66–74.
[51] Ghozatloo A, Rashidi AM, Shariaty-Niasar M. Effects of surface modification on the dispersion and thermal conductivity of CNT/water nanofluids. Int Commun Heat Mass Transf 2014;54:1–7.
[52] Sabiha M, Mostafizur R, Saidur R, Mekhilef S. Experimental investigation on thermo physical properties of single walled carbon nanotube nanofluids. Int J Heat Mass Transf 2016;93:862–71.
[53] Choi C, Yoo H, Oh J. Preparation and heat transfer properties of nanoparticle-in-transformer oil dispersions as advanced energy-efficient coolants. Curr Appl Phys 2008;8(6):710–2.

[54] Shima PD, Philip J. Role of thermal conductivity of dispersed nanoparticles on heat transfer properties of nanofluid. Ind Eng Chem Res 2014;53(2):980–8.

[55] Yu W, France DM, Routbort JL, Choi SU. Review and comparison of nanofluid thermal conductivity and heat transfer enhancements. Heat Transf Eng 2008;29(5):432–60.

[56] Akoh H, Tsukasaki Y, Yatsuya S, Tasaki A. Magnetic properties of ferromagnetic ultrafine particles prepared by vacuum evaporation on running oil substrate. J Cryst Growth 1978;45:495–500.

[57] Zhu H-T, Lin Y-S, Yin Y-S. A novel one-step chemical method for preparation of copper nanofluids. J Colloid Interface Sci 2004;277(1):100–3.

[58] Eastman J, Choi S, Li S, Yu W, Thompson L. Anomalously increased effective thermal conductivities of ethylene glycol-based nanofluids containing copper nanoparticles. Appl Phys Lett 2001;78(6):718–20.

[59] Nikkam N, Saleemi M, Haghighi EB, Ghanbarpour M, Khodabandeh R, Muhammed M, et al. Fabrication, characterization and thermo-physical property evaluation of SiC nanofluids for heat transfer applications. Nano-Micro Lett 2014;6(2).

[60] Nikkam N, Ghanbarpour M, Saleemi M, Haghighi EB, Khodabandeh R, Muhammed M, et al. Experimental investigation on thermo-physical properties of copper/diethylene glycol nanofluids fabricated via microwave-assisted route. Appl Therm Eng 2014;65(1):158–65.

[61] Zhao Y, Zhu J-J, Hong J-M, Bian N, Chen H-Y. Microwave-induced polyol-process synthesis of copper and copper oxide nanocrystals with controllable morphology. Eur J Inorg Chem 2004;2004(20):4072–80.

[62] Bönnemann H, Botha S, Bladergroen B, Linkov V. Monodisperse copper- and silver-nanocolloids suitable for heat-conductive fluids. Appl Organomet Chem 2005;19(6):768–73.

[63] Mahbubul I, Saidur R, Amalina M. Latest developments on the viscosity of nanofluids. Int J Heat Mass Transf 2012;55(4):874–85.

[64] Granqvist C, Buhrman R. Ultrafine metal particles. J Appl Phys 1976;47(5):2200–19.

[65] Beaber A, Qi L, Hafiz J, McMurry P, Heberlein J, Gerberich W, et al. Nanostructured SiC by chemical vapor deposition and nanoparticle impaction. Surf Coatings Technol 2007;202(4):871–5.

[66] Hong T-K, Yang H-S, Choi C. Study of the enhanced thermal conductivity of Fe nanofluids. J Appl Phys 2005;97(6):064311.

[67] Das SK, Putra N, Roetzel W. Pool boiling characteristics of nano-fluids. Int J Heat Mass Transf 2003;46(5):851–62.

[68] Chopkar M, Das PK, Manna I. Synthesis and characterization of nanofluid for advanced heat transfer applications. Scr Mater 2006;55(6):549–52.

[69] Pak BC, Cho YI. Hydrodynamic and heat transfer study of dispersed fluids with submicron metallic oxide particles. Exp Heat Transf: A Journal of Thermal Energy Generation, Transport, Storage, and Conversion 1998;11(2):151–70.

[70] Yu W, Xie H, Chen L, Li Y. Investigation of thermal conductivity and viscosity of ethylene glycol based ZnO nanofluid. Thermochim Acta 2009;491(1):92–6.

[71] Abbasian Arani A, Amani J. Experimental study on the effect of TiO_2–water nanofluid on heat transfer and pressure drop. Exp Therm Fluid Sci 2012;42:107–15.

[72] Hajipour M, Dehkordi AM. Mixed-convection flow of Al_2O_3–H_2O nanofluid in a channel partially filled with porous metal foam: experimental and numerical study. Exp Therm Fluid Sci 2014;53:49–56.

[73] Wang L, Fan J. Nanofluids research: key issues. Nanoscale Res Lett 2010;5(8):1241–52.

[74] Michaelides E. Nanofluidics: thermodynamic and transport properties. Cham, ZG (Switzerland): Springer; 2014 ISBN: 978-3-319-05621-0.

[75] Li X, Zhu D, Wang X. Evaluation on dispersion behavior of the aqueous copper nano-suspensions. J Colloid Interface Sci 2007;310(2):456–63.

[76] Beck MP, Yuan Y, Warrier P, Teja AS. The thermal conductivity of alumina nanofluids in water, ethylene glycol, and ethylene glycol+water mixtures. J Nanopart Res 2010;12(4):1469–77.

[77] Li X, Zhu D, Wang X, Wang N, Gao J, Li H. Thermal conductivity enhancement dependent pH and chemical surfactant for Cu–H_2O nanofluids. Thermochim Acta 2008;469(1):98–103.

[78] Tadros TF. Applied surfactants: principles and applications. Weinheim (Germany): John Wiley & Sons; 2006 ISBN: 978-3-527-30629-9.

[79] Jiang H, Li H, Xu Q, Shi L. Effective thermal conductivity of nanofluids considering interfacial nano-shells. Mater Chem Phys 2014;148(1):195–200.

[80] Yu W, Choi S. The role of interfacial layers in the enhanced thermal conductivity of nanofluids: a renovated Maxwell model. J Nanopart Res 2003;5(1–2):167–71.

[81] Yu W, Choi S. The role of interfacial layers in the enhanced thermal conductivity of nanofluids: a renovated Hamilton-crosser model. J Nanopart Res 2004;6(4):355–61.

[82] Xue Q, Xu W-M. A model of thermal conductivity of nanofluids with interfacial shells. Mater Chem Phys 2005;90(2):298–301.

[83] Li L, Zhang Y, Ma H, Yang M. Molecular dynamics simulation of effect of liquid layering around the nanoparticle on the enhanced thermal conductivity of nanofluids. J Nanopart Res 2010;12(3):811–21.

[84] Puliti G, Paolucci S, Sen M. Thermodynamic properties of gold–water nanolayer mixtures using molecular dynamics. J Nanopart Res 2011;13(9):4277–93.

[85] Chiavazzo E, Fasano M, Asinari P, Decuzzi P. Scaling behaviour for the water transport in nanoconfined geometries. Nat Commun 2014;5(4565).

[86] Fasano M, Chiavazzo E, Asinari P. Water transport control in carbon nanotube arrays. Nanoscale Res Lett 2014;9(1):1–8.

[87] Morciano M, Fasano M, Nold A, Correia Braga C, Yatsyshin P, Sibley D, et al. Mass transfer properties of nanoconfined fluids at solid–liquid interfaces: from atomistic simulations to continuum models. Bull Am Phys Soc 2015;60(21):506.

[88] Cardellini A, Fasano M, Chiavazzo E, Asinari P. Mass transport phenomena at solid-liquid nanoscale interface in biomedical applications. in: VI international conference on computational methods for coupled problems in science and engineering COUPLED PROBLEMS 2015, vol. 593. International Center for Numerical Methods in Engineering (CIMNE); Cornellà de Llobregat (Spain). ISBN: 978-84-943928-3-2, 2015.

[89] Jang SP, Choi SU. Role of Brownian motion in the enhanced thermal conductivity of nanofluids. Appl Phys Lett 2004;84(21):4316–8.

[90] Koo J, Kleinstreuer C. A new thermal conductivity model for nanofluids. J Nanopart Res 2004;6(6):577–88.

[91] Kumar DH, Patel HE, Kumar VR, Sundararajan T, Pradeep T, Das SK. Model for heat conduction in nanofluids. Phys Rev Lett 2004;93(14):144301.

[92] Prasher R, Bhattacharya P, Phelan PE. Thermal conductivity of nanoscale colloidal solutions (nanofluids). Phys Rev Lett 2005;94(2):025901.

[93] Evans W, Fish J, Keblinski P. Role of Brownian motion hydrodynamics on nanofluid thermal conductivity. Appl Phys Lett 2006;88(9):093116.

[94] Patel HE, Sundararajan T, Das SK. A cell model approach for thermal conductivity of nanofluids. J Nanopart Res 2008;10(1):87–97.

[95] Warzoha RJ, Fleischer AS. Heat flow at nanoparticle interfaces. Nano Energy 2014;6:137–58.

[96] Chiavazzo E, Asinari P. Reconstruction and modeling of 3D percolation networks of carbon fillers in a polymer matrix. Int J Therm Sci 2010;49:2272–81.

[97] Putnam SA, Cahill DG, Ash BJ, Schadler LS. High-precision thermal conductivity measurements as a probe of polymer/nanoparticle interfaces. J Appl Phys 2003;94(10):6785–8.

[98] Prasher R, Phelan PE, Bhattacharya P. Effect of aggregation kinetics on the thermal conductivity of nanoscale colloidal solutions (nanofluid). Nano Lett 2006;6(7):1529–34.

[99] Eapen J, Rusconi R, Piazza R, Yip S. The classical nature of thermal conduction in nanofluids. J Heat Transf 2010;132(10):102402.

[100] Nan C-W, Birringer R, Clarke DR, Gleiter H. Effective thermal conductivity of particulate composites with interfacial thermal resistance. J Appl Phys 1997;81(10):6692–9.

[101] Prasher R, Evans W, Meakin P, Fish J, Phelan P, Keblinski P. Effect of aggregation on thermal conduction in colloidal nanofluids. Appl Phys Lett 2006;89(14):143119.

[102] Keblinski P, Prasher R, Eapen J. Thermal conductance of nanofluids: is the controversy over?. J Nanopart Res 2008;10(7):1089–97.

[103] Buongiorno J, Venerus DC, Prabhat N, McKrell T, Townsend J, Christianson R, et al. A benchmark study on the thermal conductivity of nanofluids. J Appl Phys 2009;106(9):094312.

[104] Hashin Z, Shtrikman S. A variational approach to the theory of the effective magnetic permeability of multiphase materials. J Appl Phys 1962;33(10):3125–31.

[105] Maxwell JC. A treatise on electricity and magnetism, vol. 1. Dover (UK): Clarendon Press; 1873 ISBN: 978-0486606361.

[106] Sattler KD. Handbook of nanophysics: nanoparticles and quantum dots. Boca Raton, FL,USA: CRC Press; 2010 ISBN: 978142007544.

[107] Derjaguin B, Landau L. The theory of stability of highly charged lyophobic sols and coalescence of highly charged particles in electrolyte solutions. Acta Physicochim URSS 1941;14:633–52.

[108] Verwey E, Overbeek JTG. Theory of the stability of lyophobic colloids. J Colloid Sci 1955;10(2):224–5.

[109] Hunter RJ. Foundations of colloid science. Oxford, UK: Oxford University Press Inc.; 2001 ISBN: 978-0198505020.

[110] Israelachvili JN. Intermolecular and surface forces: revised. third edition. Amsterdam, The Netherlands: Academic Press; 2011 ISBN: 978-0123919274.

[111] Paul G, Chopkar M, Manna I, Das P. Techniques for measuring the thermal conductivity of nanofluids: a review. Renew Sustain Energy Rev 2010;14(7):1913–24.

[112] Lee S, Choi S-S, Li S, Eastman JA. Measuring thermal conductivity of fluids containing oxide nanoparticles. J Heat Transf 1999;121(2):280–9.

[113] Hwang Y, Ahn Y, Shin H, Lee C, Kim G, Park H, et al. Investigation on characteristics of thermal conductivity enhancement of nanofluids. Curr Appl Phys 2006;6(6):1068–71.

[114] Gupta SS, Siva VM, Krishnan S, Sreeprasad T, Singh PK, Pradeep T, et al. Thermal conductivity enhancement of nanofluids containing graphene nanosheets. J Appl Phys 2011;110(8):084302.

[115] Pang C, Jung J-Y, Lee JW, Kang YT. Thermal conductivity measurement of methanol-based nanofluids with Al_2O_3 and SiO_2 nanoparticles. Int J Heat Mass Transf 2012;55(21):5597–602.

[116] Garg J, Poudel B, Chiesa M, Gordon J, Ma J, Wang J, et al. Enhanced thermal conductivity and viscosity of copper nanoparticles in ethylene glycol nanofluid. J Appl Phys 2008;103(7):074301.

[117] Zhu D, Li X, Wang N, Wang X, Gao J, Li H. Dispersion behavior and thermal conductivity characteristics of Al_2O_3–H_2O nanofluids. Curr Appl Phys 2009;9(1):131–9.

[118] Wang XJ, Zhu DS, Yang S. Investigation of pH and SDBS on enhancement of thermal conductivity in nanofluids. Chem Phys Lett 2009;470(1):107–11 http://dx.doi.org/10.1016/j.cplett.2009.01.035.

[119] Das SK, Putra N, Thiesen P, Roetzel W. Temperature dependence of thermal conductivity enhancement for nanofluids. J Heat Transf 2003;125(4):567–74.

[120] Bhattacharya P, Nara S, Vijayan P, Tang T, Lai W, Phelan P, et al. Characterization of the temperature oscillation technique to measure the thermal conductivity of fluids. Int J Heat Mass Transf 2006;49(17):2950–6.

[121] Oh D-W, Jain A, Eaton JK, Goodson KE, Lee JS. Thermal conductivity measurement and sedimentation detection of aluminum oxide nanofluids by using the 3ω method. Int J Heat Fluid Flow 2008;29(5):1456–61.

[122] Wang X, Xu X, Choi SUS. Thermal conductivity of nanoparticle–fluid mixture. J Thermophys Heat Transf 1999;13(4):474–80.

[123] Kurt H, Kayfeci M. Prediction of thermal conductivity of ethylene glycol–water solutions by using artificial neural networks. Appl Energy 2009;86 (10):2244–8.

[124] Li CH, Williams W, Buongiorno J, Hu L-W, Peterson G. Transient and steady-state experimental comparison study of effective thermal conductivity of Al_2O_3/water nanofluids. J Heat Transf 2008;130(4):042407.

[125] Hong SW, Kang Y-T, Kleinstreuer C, Koo J. Impact analysis of natural convection on thermal conductivity measurements of nanofluids using the transient hot-wire method. Int J Heat Mass Transf 2011;54(15):3448–56.

[126] Fang K-C, Weng C-I, Ju S-P. An investigation into the structural features and thermal conductivity of silicon nanoparticles using molecular dynamics simulations. Nanotechnology 2006;17(15):3909.

[127] Beck MP, Yuan Y, Warrier P, Teja AS. The effect of particle size on the thermal conductivity of alumina nanofluids. J Nanopart Res 2009;11(5):1129–36.

[128] Warrier P, Yuan Y, Beck MP, Teja AS. Heat transfer in nanoparticle suspensions: modeling the thermal conductivity of nanofluids. AIChE J 2010;56 (12):3243–56.

[129] Beck MP, Yuan Y, Warrier P, Teja AS. The thermal conductivity of aqueous nanofluids containing ceria nanoparticles. J Appl Phys 2010;107(6):066101.

[130] Timofeeva EV, Smith DS, Yu W, France DM, Singh D, Routbort JL. Particle size and interfacial effects on thermo-physical and heat transfer characteristics of water-based α-SiC nanofluids. Nanotechnology 2010;21(21):215703.

[131] Fasano M, Bozorg Bigdeli M, Vaziri Sereshk MR, Chiavazzo E, Asinari P. Thermal transmittance of carbon nanotube networks: guidelines for novel thermal storage systems and polymeric material of thermal interest. Renew Sustain Energy Rev 2015;41:1028–36.

[132] Philip J, Shima P, Raj B. Evidence for enhanced thermal conduction through percolating structures in nanofluids. Nanotechnology 2008;19(30):305706.

[133] Shima P, Philip J, Raj B. Role of microconvection induced by Brownian motion of nanoparticles in the enhanced thermal conductivity of stable nanofluids. Appl Phys Lett 2009;94(22):223101.

[134] Teng T-P, Hung Y-H, Teng T-C, Mo H-E, Hsu H-G. The effect of alumina/water nanofluid particle size on thermal conductivity. Appl Therm Eng 2010;30(14–15):2213–8.

[135] Pastoriza-Gallego M, Casanova C, Páramo R, Barbés B, Legido J, Piñeiro M. A study on stability and thermophysical properties (density and viscosity) of Al_2O_3 in water nanofluid. J Appl Phys 2009;106(6):064301.

[136] Wamkam CT, Opoku MK, Hong H, Smith P. Effects of pH on heat transfer nanofluids containing ZrO_2 and TiO_2 nanoparticles. J Appl Phys 2011;109 (2):024305.

[137] Younes H, Christensen G, Luan X, Hong H, Smith P. Effects of alignment, pH, surfactant, and solvent on heat transfer nanofluids containing Fe_2O_3 and CuO nanoparticles. J Appl Phys 2012;111(6):064308.

[138] Ismay MJ, Doroodchi E, Moghtaderi B. Effects of colloidal properties on sensible heat transfer in water-based titania nanofluids. Chem Eng Res Des 2013;91(3):426–36.

[139] Lee D, Kim J-W, Kim BG. A new parameter to control heat transport in nanofluids: surface charge state of the particle in suspension. J Phys Chem B 2006;110(9):4323–8.

[140] Lee SW, Park SD, Kang S, Bang IC, Kim JH. Investigation of viscosity and thermal conductivity of SiC nanofluids for heat transfer applications. Int J Heat Mass Transf 2011;54(1):433–8.

[141] Cao F, Liu Y, Xu J, He Y, Hammouda B, Qiao R, et al. Probing nanoscale thermal transport in surfactant solutions. Sci Rep 2015;5.

[142] Choi S, Zhang Z, Yu W, Lockwood F, Grulke E. Anomalous thermal conductivity enhancement in nanotube suspensions. Appl Phys Lett 2001;79 (14):2252–4.

[143] Shaikh S, Lafdi K, Ponnappan R. Thermal conductivity improvement in carbon nanoparticle doped PAO oil: an experimental study. J Appl Phys 2007;101(6):064302.

[144] Li CH, Peterson G. Experimental investigation of temperature and volume fraction variations on the effective thermal conductivity of nanoparticle suspensions (nanofluids). J Appl Phys 2006;99(8):084314.

[145] Patel HE, Anoop K, Sundararajan T, Das SK. A micro-convection model for thermal conductivity of nanofluids. in: International heat transfer conference. Begel House Inc.; 2006. p. 863–9, 13th INTERNATIONAL HEAT TRANSFER CONFERENCE, Sydney, Australia, 13 – 18 August 2006. ISSN: 1-56700-225-0.

[146] Murshed S, Leong K, Yang C. Investigations of thermal conductivity and viscosity of nanofluids. Int J Therm Sci 2008;47(5):560–8.

[147] Mintsa HA, Roy G, Nguyen CT, Doucet D. New temperature dependent thermal conductivity data for water-based nanofluids. Int J Therm Sci 2009;48(2):363–71.

[148] Vajjha RS, Das DK. Experimental determination of thermal conductivity of three nanofluids and development of new correlations. Int J Heat Mass Transf 2009;52(21):4675–82.

[149] Duangthongsuk W, Wongwises S. Measurement of temperature-dependent thermal conductivity and viscosity of TiO_2–water nanofluids. Exp Therm Fluid Sci 2009;33(4):706–14.

[150] Philip J, Shima P, Raj B. Nanofluid with tunable thermal properties. Appl Phys Lett 2008;92(4):043108-1–3.

[151] Shima P, Philip J, Raj B. Magnetically controllable nanofluid with tunable thermal conductivity and viscosity. Appl Phys Lett 2009;95(13):133112-1–3.

[152] Eastman JA, Phillpot S, Choi S, Keblinski P. Thermal transport in nanofluids 1. Annu Rev Mater Res 2004;34:219–46.

[153] Patel HE, Sundararajan T, Das SK. An experimental investigation into the thermal conductivity enhancement in oxide and metallic nanofluids. J Nanopart Res 2010;12(3):1015–31.

[154] Ijam A, Saidur R. Nanofluid as a coolant for electronic devices (cooling of electronic devices). Appl Therm Eng 2012;32:76–82.

[155] Liu M, Lin MC, Wang C. Enhancements of thermal conductivities with Cu, CuO, and carbon nanotube nanofluids and application of MWNT/water nanofluid on a water chiller system. Nanoscale Res Lett 2011;6(1):1–13.

[156] Hwang Y, Park H, Lee J, Jung W. Thermal conductivity and lubrication characteristics of nanofluids. Curr Appl Phys 2006;6:e67–71.

[157] Nikkam N, Haghighi EB, Saleemi M, Behi M, Khodabandeh R, Muhammed M, et al. Experimental study on preparation and base liquid effect on thermo-physical and heat transport characteristics of α-SiC nanofluids. Int Commun Heat Mass Transf 2014;55:38–44.

[158] Timofeeva EV, Gavrilov AN, McCloskey JM, Tolmachev YV, Sprunt S, Lopatina LM, et al. Thermal conductivity and particle agglomeration in alumina nanofluids: experiment and theory. Phys Rev E 2007;76(6):061203.

[159] Jackson RG, Kahani M, Karwa N, Wu A, Lamb R, Taylor R, et al. Effect of surface wettability on carbon nanotube water-based nanofluid droplet impingement heat transfer. J Phys: Conf Ser 2014;525:012024.

[160] Harish S, Ishikawa K, Einarsson E, Aikawa S, Inoue T, Zhao P, et al. Temperature dependent thermal conductivity increase of aqueous nanofluid with single walled carbon nanotube inclusion. Mater Express 2012;2(3):213–23.

[161] Corcione M. Empirical correlating equations for predicting the effective thermal conductivity and dynamic viscosity of nanofluids. Energy Convers Manag 2011;52(1):789–93.

[162] Chon CH, Kihm KD, Lee SP, Choi SU. Empirical correlation finding the role of temperature and particle size for nanofluid (Al_2O_3) thermal conductivity enhancement. Appl Phys Lett 2005;87(15):153107-1–3.

[163] Timofeeva EV, Routbort JL, Singh D. Particle shape effects on thermophysical properties of alumina nanofluids. J Appl Phys 2009;106(1):014304.

[164] Pang C, Lee JW, Hong H, Kang YT. Heat conduction mechanism in nanofluids. J Mech Sci Technol 2014;28(7):2925–36.

[165] Khanafer K, Vafai K. A critical synthesis of thermophysical characteristics of nanofluids. Int J Heat Mass Transf 2011;54(19–20):4410–28.

[166] Hamilton R, Crosser O. Thermal conductivity of heterogeneous two-component systems. Ind Eng Chem Fundam 1962;1(3):187–91.

[167] Jeffrey DJ. Conduction through a random suspension of spheres. Proc R Soc Lond A. Math Phys Sci 1973;335(1602):355–67.

[168] Vajjha R, Das D, Namburu P. Numerical study of fluid dynamic and heat transfer performance of Al_2O_3 and CuO nanofluids in the flat tubes of a radiator. Int J Heat Fluid Flow 2010;31(4):613–21.

[169] Corcione M. Rayleigh–Bénard convection heat transfer in nanoparticle suspensions. Int J Heat Fluid Flow 2011;32(1):65–77.

[170] Ghadimi A, Saidur R, Metselaar H. A review of nanofluid stability properties and characterization in stationary conditions. Int J Heat Mass Transf 2011;54 (17–18):4051–68.

[171] Rajabpour A, Akizi FY, Heyhat MM, Gordiz K. Molecular dynamics simulation of the specific heat capacity of water–Cu nanofluids. Int Nano Lett 2013;3 (1):58.

[172] Yang Y, Zhang ZG, Grulke EA, Anderson WB, Wu G. Heat transfer properties of nanoparticle-in-fluid dispersions (nanofluids) in laminar flow. Int J Heat Mass Transf 2005;48(6):1107–16.

[173] Zhou S-Q, Ni R. Measurement of the specific heat capacity of water-based Al_2O_3 nanofluid. Appl Phys Lett 2008;92(9):093123-1–3.

[174] Pantzali M, Kanaris A, Antoniadis K, Mouza A, Paras S. Effect of nanofluids on the performance of a miniature plate heat exchanger with modulated surface. Int J Heat Fluid Flow 2009;30(4):691–9.

[175] Starace AK, Gomez JC, Wang J, Pradhan S, Glatzmaier GC. Nanofluid heat capacities. J Appl Phys 2011;110(12):124323.

[176] Kumaresan V, Velraj R. Experimental investigation of the thermo-physical properties of water–ethylene glycol mixture based CNT nanofluids. Thermochim Acta 2012;545:180–6.

[177] Saeedinia M, Akhavan-Behabadi M, Razi P. Thermal and rheological characteristics of CuO-Base oil nanofluid flow inside a circular tube. Int Commun Heat Mass Transf 2012;39(1):152–9.

[178] Elias M, Mahbubul I, Saidur R, Sohel M, Shahrul I, Khaleduzzaman S, et al. Experimental investigation on the thermo-physical properties of Al_2O_3 nanoparticles suspended in car radiator coolant. Int Commun Heat Mass Transf 2014;54:48–53.

[179] Vajjha RS, Das DK. Specific heat measurement of three nanofluids and development of new correlations. J Heat Transf 2009;131(7):071601.

[180] Murshed SS. Simultaneous measurement of thermal conductivity, thermal diffusivity, and specific heat of nanofluids. Heat Transf Eng 2012;33(8):722–31.

[181] Kulkarni DP, Vajjha RS, Das DK, Oliva D. Application of aluminum oxide nanofluids in diesel electric generator as jacket water coolant. Appl Therm Eng 2008;28(14):1774–81.

[182] Fakoor Pakdaman M, Akhavan-Behabadi M, Razi P. An experimental investigation on thermo-physical properties and overall performance of MWCNT/heat transfer oil nanofluid flow inside vertical helically coiled tubes. Exp Therm Fluid Sci 2012;40:103–11.

[183] Pandey SD, Nema V. Experimental analysis of heat transfer and friction factor of nanofluid as a coolant in a corrugated plate heat exchanger. Exp Therm Fluid Sci 2012;38:248–56.

[184] Robertis ED, Cosme E, Neves R, Kuznetsov A, Campos A, Landi S, et al. Application of the modulated temperature differential scanning calorimetry technique for the determination of the specific heat of copper nanofluids. Appl Therm Eng 2012;41:10–7 In: 13th Brazilian congress of thermal sciences and engineering.

[185] Wang B-X, Zhou L-P, Peng X-F. Surface and size effects on the specific heat capacity of nanoparticles. Int J Thermophys 2006;27(1):139–51.

[186] He Q, Wang S, Tong M, Liu Y. Experimental study on thermophysical properties of nanofluids as phase-change material (PCM) in low temperature cool storage. Energy Convers Manag 2012;64:199–205.

[187] Shahrul I, Mahbubul I, Khaleduzzaman S, Saidur R, Sabri M. A comparative review on the specific heat of nanofluids for energy perspective. Renew Sustain Energy Rev 2014;38:88–98.

[188] Amrollahi A, Hamidi A, Rashidi A. The effects of temperature, volume fraction and vibration time on the thermo-physical properties of a carbon nanotube suspension (carbon nanofluid). Nanotechnology 2008;19(31):315701.

[189] Xuan Y, Roetzel W. Conceptions for heat transfer correlation of nanofluids. Int J Heat Mass Transf 2000;43(19):3701–7.

[190] O'Hanley H, Buongiorno J, McKrell T, Hu L-W. Measurement and model validation of nanofluid specific heat capacity with differential scanning calorimetry. In: Advances in mechanical engineering; 2012.

[191] Murshed SS. Determination of effective specific heat of nanofluids. J Exp Nanosci 2011;6(5):539–46.

[192] Teng T-P, Hung Y-H. Estimation and experimental study of the density and specific heat for alumina nanofluid. J Exp Nanosci 2012;9(7):707–18.

[193] Ho C-J, Chen M, Li Z. Numerical simulation of natural convection of nanofluid in a square enclosure: effects due to uncertainties of viscosity and thermal conductivity. Int J Heat Mass Transf 2008;51(17):4506–16.

[194] Khanafer K, Vafai K, Lightstone M. Buoyancy-driven heat transfer enhancement in a two-dimensional enclosure utilizing nanofluids. Int J Heat Mass Transf 2003;46(19):3639–53.

[195] Ho C, Liu W, Chang Y, Lin C. Natural convection heat transfer of alumina–water nanofluid in vertical square enclosures: an experimental study. Int J Therm Sci 2010;49(8):1345–53.

[196] Chandrasekar M, Suresh S, Chandra Bose A. Experimental investigations and theoretical determination of thermal conductivity and viscosity of Al_2O_3/water nanofluid. Exp Therm Fluid Sci 2010;34(2):210–6.

[197] Xian-Ju W, Xin-Fang L. Influence of pH on nanofluids' viscosity and thermal conductivity. Chin Phys Lett 2009;26(5):056601.

[198] Nguyen C, Desgranges F, Roy G, Galanis N, Maré T, Boucher S. Temperature and particle-size dependent viscosity data for water-based nanofluids—hysteresis phenomenon. Int J Heat Fluid Flow 2007;28(6):1492–506.

[199] Kang YJ, Yang S. Integrated microfluidic viscometer equipped with fluid temperature controller for measurement of viscosity in complex fluids. Microfluid Nanofluid 2013;14(3–4):657–68.

[200] Einstein A. Eine neue bestimmung der moleküldimensionen. Ann Phys 1906;324(2):289–306.

[201] Krieger IM, Dougherty TJ. A mechanism for non-Newtonian flow in suspensions of rigid spheres. Trans Soc Rheol 1959;3(1):137–52.

[202] Egan V, Walsh P, Walsh E. On viscosity measurements of nanofluids in micro and mini tube flow. J Phys D: Appl Phys 2009;42(16):165502.

[203] Jang SP, Lee J-H, Hwang KS, Choi SU. Particle concentration and tube size dependence of viscosities of Al_2O_3–water nanofluids flowing through micro- and minitubes. Appl Phys Lett 2007;91(24):243112-1–3.

[204] Ayela F, Chevalier J. Comment on particle concentration and tube size dependence of viscosities of Al_2O_3–water nanofluids flowing through micro- and minitubes. Appl Phys Lett 2007;91:243112;
Ayela F, Chevalier J. Comment on particle concentration and tube size dependence of viscosities of Al_2O_3–water nanofluids flowing through micro- and minitubes. Appl Phys Lett 2009;94(6) 066101–066101.

[205] Heine DR, Petersen MK, Grest GS. Effect of particle shape and charge on bulk rheology of nanoparticle suspensions. J Chem Phys 2010;132(18):184509.

[206] Santamara-Holek I, Mendoza CI. The rheology of concentrated suspensions of arbitrarily-shaped particles. J Colloid Interface Sci 2010;346(1):118–26.

[207] Rao Y. Nanofluids: stability, phase diagram, rheology and applications. Particuology 2010;8(6):549–55.

[208] Prasher R, Song D, Wang J, Phelan P. Measurements of nanofluid viscosity and its implications for thermal applications. Appl Phys Lett 2006;89(13):133108.

[209] Mena JB, Ubices de Moraes AA, Benito YR, Ribatski G, Parise JAR. Extrapolation of Al_2O_3–water nanofluid viscosity for temperatures and volume concentrations beyond the range of validity of existing correlations. Appl Therm Eng 2013;51(1):1092–7.

[210] Yu W, Xie H, Li Y, Chen L. Experimental investigation on thermal conductivity and viscosity of aluminum nitride nanofluid. Particuology 2011;9(2):187–91.

[211] Kim S, Kim C, Lee W-H, Park S-R. Rheological properties of alumina nanofluids and their implication to the heat transfer enhancement mechanism. J Appl Phys 2011;110(3):034316.

[212] Phuoc TX, Massoudi M, Chen R-H. Viscosity and thermal conductivity of nanofluids containing multi-walled carbon nanotubes stabilized by chitosan. Int J Therm Sci 2011;50(1):12–8.

[213] Mingzheng Z, Guodong X, Jian L, Lei C, Lijun Z. Analysis of factors influencing thermal conductivity and viscosity in different kinds of surfactant solutions. Exp Therm Fluid Sci 2012;36:22–9.

[214] Timofeeva EV, Moravek MR, Singh D. Improving the heat transfer efficiency of synthetic oil with silica nanoparticles. J Colloid Interface Sci 2011;364(1):71–9.

[215] Kamranfar P, Jamialahmadi M. Effect of surfactant micelle shape transition on the microemulsion viscosity and its application in enhanced oil recovery processes. J Mol Liquids 2014;198:286–91, http://dx.doi.org/10.1016/j.molliq.2014.07.009.

[216] Nguyen C, Desgranges F, Galanis N, Roy G, Maré T, Boucher S, et al. Viscosity data for Al_2O_3–water nanofluid-hysteresis: is heat transfer enhancement using nanofluids reliable?. Int J Therm Sci 2008;47(2):103–11.

[217] Lu W-Q, Fan Q-M. Study for the particle's scale effect on some thermophysical properties of nanofluids by a simplified molecular dynamics method. Eng Anal Bound Elem 2008;32(4):282–9.

[218] Pastoriza-Gallego M, Casanova C, Legido J, Piñeiro M. CuO in water nanofluid: influence of particle size and polydispersity on volumetric behaviour and viscosity. Fluid Phase Equilibria 2011;300(1–2):188–96.

[219] Rudyak VY, Krasnolutskii S. Dependence of the viscosity of nanofluids on nanoparticle size and material. Phys Lett A 2014;378(26):1845–9.

[220] He Y, Jin Y, Chen H, Ding Y, Cang D, Lu H. Heat transfer and flow behaviour of aqueous suspensions of TiO_2 nanoparticles (nanofluids) flowing upward through a vertical pipe. Int J Heat Mass Transf 2007;50(11–12):2272–81.

[221] Sahoo BC, Vajjha RS, Ganguli R, Chukwu GA, Das DK. Determination of rheological behavior of aluminum oxide nanofluid and development of new viscosity correlations. Pet Sci Technol 2009;27(15):1757–70.

[222] Godson L, Raja B, Lal DM, Wongwises S. Experimental investigation on the thermal conductivity and viscosity of silver-deionized water nanofluid. Exp Heat Transf 2010;23(4):317–32.

[223] Hemmat Esfe M, Saedodin S. An experimental investigation and new correlation of viscosity of ZnO–EG nanofluid at various temperatures and different solid volume fractions. Exp Therm Fluid Sci 2014;55:1–5.

[224] Ghanbarpour M, Bitaraf Haghigi E, Khodabandeh R. Thermal properties and rheological behavior of water based Al_2O_3 nanofluid as a heat transfer fluid. Exp Therm Fluid Sci 2014;53:227–35.

[225] Meybodi MK, Daryasafar A, Koochi MM, Moghadasi J, Meybodi RB, Ghahfarokhi AK. A novel correlation approach for viscosity prediction of water based nanofluids of Al_2O_3, TiO_2, SiO_2 and CuO. J Taiwan Inst Chem Eng 2016;58:19–27.

[226] Tseng WJ, Lin K-C. Rheology and colloidal structure of aqueous TiO_2 nanoparticle suspensions. Mater Sci Eng: A 2003;355(12):186–92.

[227] Namburu P, Kulkarni D, Dandekar A, Das D. Experimental investigation of viscosity and specific heat of silicon dioxide nanofluids. MicroNano Lett IET 2007;2(3):67–71.

[228] Kulkarni DP, Das DK, Vajjha RS. Application of nanofluids in heating buildings and reducing pollution. Appl Energy 2009;86(12):2566–73.

[229] Namburu PK, Kulkarni DP, Misra D, Das DK. Viscosity of copper oxide nanoparticles dispersed in ethylene glycol and water mixture. Exp Therm Fluid Sci 2007;32(2):397–402.

[230] Putra N, Roetzel W, Das SK. Natural convection of nano-fluids. Heat Mass Transf 2003;39(8–9):775–84.

[231] Anoop K, Kabelac S, Sundararajan T, Das SK. Rheological and flow characteristics of nanofluids: influence of electroviscous effects and particle agglomeration. J Appl Phys 2009;106(3):034909.

[232] Batchelor G. The effect of Brownian motion on the bulk stress in a suspension of spherical particles. J Fluid Mech 1977;83(01):97–117.

[233] Brinkman HC. The viscosity of concentrated suspensions and solutions. J Chem Phys 1952;20(4):571–81.

[234] Lundgren TS. Slow flow through stationary random beds and suspensions of spheres. J Fluid Mech 1972;51(02):273–99.

[235] Frankel N, Acrivos A. On the viscosity of a concentrated suspension of solid spheres. Chem Eng Sci 1967;22(6):847–53.

[236] Chen H, Ding Y, He Y, Tan C. Rheological behaviour of ethylene glycol based titania nanofluids. Chem Phys Lett 2007;444(4–6):333–7 [cited By (since 1996) 105].

[237] Kitano T, Kataoka T, Shirota T. An empirical equation of the relative viscosity of polymer melts filled with various inorganic fillers. Rheol Acta 1981;20(2):207–9.

[238] Graham AL. On the viscosity of suspensions of solid spheres. Appl Sci Res 1981;37(3–4):275–86.

[239] Masoumi N, Sohrabi N, Behzadmehr A. A new model for calculating the effective viscosity of nanofluids. J Phys D: Appl Phys 2009;42(5):055501.

[240] Longo GA, Zilio C, Ceseracciu E, Reggiani M. Application of artificial neural network (ANN) for the prediction of thermal conductivity of oxide-water nanofluids. Nano Energy 2012;1(2):290–6.

[241] Vajjha R, Das D, Mahagaonkar B. Density measurement of different nanofluids and their comparison with theory. Pet Sci Technol 2009;27(6):612–24.

[242] Servati V AA, Javaherdeh K, Ashorynejad HR. Magnetic field effects on force convection flow of a nanofluid in a channel partially filled with porous media using lattice Boltzmann method. Adv Powder Technol 2014;25(2):666–75.
[243] Incropera FP. Liquid cooling of electronic devices by single-phase convection, 3. Weinheim, Germany: Wiley-Interscience; 1999 ISBN: 978-0471159865.
[244] ASHRAE A. Handbook of fundamentals. Atlanta, GA: American Society of Heating Refrigerating and Air Conditioning Engineers; 2013.
[245] McQuiston F, Parker J, Spitler J. Heating, ventilating, and air conditioning: analysis and design. Weinheim ,Germany: John Wiley & Sons; 2005 ISBN: 978-0471470151.
[246] Bianco V, Nardini S, Manca O. Enhancement of heat transfer and entropy generation analysis of nanofluids turbulent convection flow in square section tubes. Nanoscale Res Lett 2011;6(1):1–12.
[247] Li Y, Fernández-Seara J, Du K, Pardiñas ÁÁ, Latas LL, Jiang W. Experimental investigation on heat transfer and pressure drop of ZnO/ethylene glycol–water nanofluids in transition flow. Appl Therm Eng 2016;93:537–48.
[248] Razi P, Akhavan-Behabadi M, Saeedinia M. Pressure drop and thermal characteristics of CuO-base oil nanofluid laminar flow in flattened tubes under constant heat flux. Int Commun Heat Mass Transf 2011;38(7):964–71.
[249] Bejan A. Heat transfer. Weinheim, Germany: John Wiley & Sons Inc; 1993 ISBN: 978-0471502906.
[250] Gnielinski V. New equations for heat and mass-transfer in turbulent pipe and channel flow. Int Chem Eng 1976;16(2):359–68.
[251] Vajjha RS, Das DK, Kulkarni DP. Development of new correlations for convective heat transfer and friction factor in turbulent regime for nanofluids. Int J Heat Mass Transf 2010;53(21):4607–18.
[252] Ferrouillat S, Bontemps A, Poncelet O, Soriano O, Gruss J-A. Influence of nanoparticle shape factor on convective heat transfer and energetic performance of water-based SiO_2 and ZnO nanofluids. Appl Therm Eng 2013;51(1):839–51.
[253] Bai M, Xu Z, Lv J. Application of nanofluids in engine cooling system. Technical report. SAE Technical Paper; 2008.
[254] Peyghambarzadeh S, Hashemabadi S, Hoseini S, Seifi Jamnani M. Experimental study of heat transfer enhancement using water/ethylene glycol based nanofluids as a new coolant for car radiators. Int Commun Heat Mass Transf 2011;38(9):1283–90.
[255] Huminic G, Huminic A. Numerical analysis of laminar flow heat transfer of nanofluids in a flattened tube. Int Commun Heat Mass Transf 2013;44:52–7.
[256] Hussein AM, Bakar R, Kadirgama K, Sharma K. Experimental measurement of nanofluids thermal properties. Diamond 2013;380(237):390.
[257] Ailor W. Engine coolant testing: state of the art. ASTM STP 705, American Society for Testing and Materials; 1980.
[258] Ghadimi A, Metselaar IH. The influence of surfactant and ultrasonic processing on improvement of stability, thermal conductivity and viscosity of titania nanofluid. Exp Therm Fluid Sci 2013;51:1–9.
[259] Ciuffini A, Scattina A, Carena F, Roberti, M, Toscano Rivalta G, Chiavazzo E, Fasano, M, Asinari P. Multi-scale computational fluid dynamics methodology for predicting thermal performance of compact heat exchanges, ASME, http://dx.doi.org/http://dx.doi.org.10.1115/1.4032980, in press.
[260] Fasano Matteo, Borri Daniele, Chiavazzo Eliodoro. Protocols for atomistic modeling of water uptake into zeolite crystals for thermal storage and other applications. Applied Thermal Enginnering, http://dx.doi.org/10.1016/j.applthermaleng.2016.02.015, in press.
[261] Annalisa Cardellini, Matteo Fasano, Eliodoro Chiavazzo, Pietro Asinari, Interfacial water thickness at inorganic nanoconstructs and biomolecules: Size matters, Physica letters A, http://dx.doi.org/10.1016/j.physleta.2016.03.015.